LBL-29214

Lawrence Berkeley Laboratory

UNIVERSITY OF CALIFORNIA

Materials & Chemical Sciences Division

Powder Processing of Aluminides

O. Kanou
(M.S. Thesis)

May 1990

LOAN COPY
Circulates
for 2 weeks
Bldg. 50 Library.
LBL-29214
Copy 2

Prepared for the U.S. Department of Energy under Contract Number DE-AC03-76SF00098.

DISCLAIMER

This document was prepared as an account of work sponsored by the United States Government. While this document is believed to contain correct information, neither the United States Government nor any agency thereof, nor the Regents of the University of California, nor any of their employees, makes any warranty, express or implied, or assumes any legal responsibility for the accuracy, completeness, or usefulness of any information, apparatus, product, or process disclosed, or represents that its use would not infringe privately owned rights. Reference herein to any specific commercial product, process, or service by its trade name, trademark, manufacturer, or otherwise, does not necessarily constitute or imply its endorsement, recommendation, or favoring by the United States Government or any agency thereof, or the Regents of the University of California. The views and opinions of authors expressed herein do not necessarily state or reflect those of the United States Government or any agency thereof or the Regents of the University of California.

Powder Processing of Aluminides

Osamu Kanou

(M.S. Thesis)

Dept. of Materials Science and Mineral Engineering
University of California,Berkeley

and
Center for Advanced Materials
Materials and Chemical Science Division
Lawrence Berkeley Laboratory
University of California
Berkeley, CA 94720

May, 1990

This work was supported by the division of Materials Science, Office of Basic Energy Research, United States Department of Energy, under contract No. DE-AC0376SF00098 with the Lawrence Berkeley Laboratory.

Powder Processing of Aluminides

by

Osamu Kanou

ABSTRACT

This research was carried out to clarify the process variables in producing Nb_3Al/Nb composite material and to examine the usefulness of Nb phase as a reinforcement in this material.

Two processes were investigated and it has been found that the synthesis and hot pressing method was suitable to produce highly densified Nb_3Al/Nb composite material. The hot pressed and heat treated specimen were examined by SEM, EDXS, X-ray diffraction and micro indentation. It has been found that the specimen consisted of a Nb_3Al matrix and a Nb phase. Cracking was strongly influenced by the Nb phases: both crack formation and crack propagation were inhibited by the Nb phases. This effect was more evident in the specimen which contained more Nb phases. It has been concluded that the usefulness of dispersed Nb phase as a reinforcement in the brittle matrix has been proven.

Table of Contents

ABSTRACT (paged separately) 1

Acknowledgements iv

1. **Introduction** 1

2. **Background**

2-1. Intermetallic Aluminides 3

2-1-1. Ni_3Al 3

2-1-2. Ti_3Al and TiAl 5

2-2. Toughening of Aluminides 6

2-3. Toughening by Dispersion of Ductile Particles .. 7

2-4. Fracture Mechanics in Composites 11

2-5. A-15 Compounds 12

3. **Experimental Procedure**

3-1. Raw Materials 13

3-2. Preparation of Fine Nb Powder 13

3-3. Mixing 14

3-4. Consolidation 14

3-5 Characterization 15

4. **Results**

4-1. Cold Compaction and Reactive Sintering 16

4-2. Synthesis 16

4-3. Hot Pressing 17

4-4. Toughness 20

5. **Discussion**

5-1. Processing 22

5-2. Evaluation of the Toughness 24

6. **Conclusion** 27

References 28

Tables 32

Figures 35

Acknowledgements

The author would like to express his appreciation to everybody who helped in completing this thesis. Especially, my thesis advisor, Professor Lutgard C. De Jonghe deserves special gratitude for his constant advise and useful discussion. And Professors, R.O. Ritchie and J. W. Morris Jr are also thanked for accepting to be a member of the thesis commitee.

I also thank LBL staff, John Holthuis, James Wu, John Jacobson and Erlene Fong Mah. I owe a lot to them in completing the experiments.

Finally, I would like to thank the members of my research group who helped me in detail.

1. Introduction

Currently, the operating temperature limit of gas-turbine engines is set by thermal constraints on materials. Since the Carnot efficiency (best efficiency obtained under adiabatic condition) is given as

$$\eta = 1 - T_1/T_2 \quad \cdots\cdots (1)$$

where T_2 is the engine operating temperature and T_1 is the reservoir temperature, the increase of operating temperature is essential to get higher efficiency. However, the currently utilized nickel-base superalloys are unlikely to meet the performance needs of the high efficiency engines. Therefore, high efficiency engines for the 21st century will require new materials which can withstand use at high stress levels at much higher temperatures. Such materials are only now conceived and under investigation for practical use. Possible candidates which can substitute for the nickel-base superalloys are intermetallic compounds, especially the intermetallic aluminides.

Aluminides, such as Ni_3Al, TiAl and Ti_3Al have been investigated for a long time because they may possess very favorable mechanical and chemical properties at temperatures above 600°C and up to 900°C, and keep better mechanical properties than superalloys above 900°C. Because practical application of intermetallics is seriously imited by their intrinsic brittleness at ambient temperature, many researchers have been stimulated to continue the investigation of these materials to improve their fracture toughness. Such investigations seem to be devided into two groups

according to the exploited toughening mechanism. One is microalloying and the other is fabricating a composite.

Metal Matrix Composite (MMC) or Ceramic Matrix Composite (CMC) are common approaches to modify the mechanical properties of matrices. Higher stiffness and higher strength are possible in MMC than in a monolithic metal. And CMC seems to be a very promising approach to produce tough materials from brittle ones. Several toughening models have been proposed, and the usefulness of these models has been demonstrated by several examples which succeeded in toughening the brittle materials.

Toughening by a dispersed ductile phase was examined in this research. Nb_3Al and Nb were chosen as a brittle intermetallic aluminide and as a ductile reinforcement, respectively. Since the fracture behavior of Nb_3Al has not been reported before, the author hopes this research can contribute to the understanding of the fracture behavior of Ni_3Al/Nb composite material and its relation to processing.

2. Background

2-1. Intermetallic Aluminides

As far as the author knows, intermetallic aluminides came first to attention as promising high-temperature structural materials following the report of Aoki *et al* on Ni_3Al [1]. Before this report, intermetallic aluminides, including Ni_3Al, Ti_3Al and TiAl had not been considered as practical materials at all due to their extreme brittleness at room temperature, although superior mechanical properties at elevated temperatures had been reported [2][3][4]. Aoki *et al* [1] reported that small addition of Boron increased the elongation to fracture of Ni_3Al up to 50%. After this report, the nature of brittleness became a subject of investigation worldwide; nevertheless, the precise role of Boron remains unclear.

Although the description of the chronological development on aluminides is not the purpose of this section, the nature of brittleness and its remedies in Ni_3Al, TiAl and Ti_3Al will be briefly reviewed.

2-1-1. Ni_3Al

Generally, brittleness can follow from these four reasons [5].

(1) Intrinsic crystallographic resistance to slip.

(2) Insufficient number of slip systems.

(3) Segregation to grain boundaries.

(4) Grain boundary structure itself.

(1) and (2) are corollary to von-Mises's criterion which requires more than 5 independant slip systems to permit extensive plasticity in polycrystals. The brittleness of some intermetallics of complicated crystal structures can be attributed to (1), because they intrinsically do not have easy slip systems. In such intrinsically brittle intermetallics, crack nucleation and propagation is the preferred deformation mode. The brittleness of NiAl (B2 structure) is explained by (2). Though this material is sufficiently simple, it is considered not to satisfy von Mises's criterion because slip may actually occur only on one special plane. However, the brittleness of Ni_3Al can not be explained by (1) and (2).

Phosphorus and Sulfur in steel are typical examples of (3), which are well known to deteriorate the toughness of steel. However, this possibility was also discarded for Ni_3Al based on the following two experimental facts; 1) a highly pure material prepared from a melt of high purity raw materials still showed brittleness [6], and 2) no evidence of impurity segregation was obtained by detailed surface analysis [7][8].

Takasugi *et al* [9] proposed that the brittleness might be caused by special bonding behavior at grain boundary. Ni_3Al has the ordered $L1_2$ (A_3B) structure. Computer calculation showed that the bonding of the $L1_2$ (A_3B) structure was quite different in grain boundaries in which A-A (Ni-Ni) metallic bonding was more dominant than A-B (Ni-Al) covalent bonding [9]. This means that a difference exists in electron density between the grain boundary and the matrix. So, Takasugi *et al* supposed that the change of the electron

density in the grain boundary was the true reason of brittleness [9]. This would be an intrinsic property in A_3B ordered alloys. According to their proposal, the improvement in elongation to fracture caused by Boron addition can be explained by the view that the electron density in the grain boundary is modified by Boron addition.

Takasugi *et al* tested the influences of third element additions and stoichometry on ductility and correlated them with the electron density change caused by third element additions and the deviation from the stoichiometic composition [10][11]. They obtained data which showed good agreement with the hypothesis. Therefore, microalloying is one attractive remedy to increase the ductility of Ni_3Al alloys.

2-1-2. TiAl and Ti_3Al

The brittleness in Titanium aluminide is considered to be caused by the sessile nature of the dislocations [12][13]. According to Lipsitt *et al* [12], the a/6[112] partial dislocation is the only one which is observed by TEM in TiAl ($L1_0$ structure). A a/6[112] partial dislocation is essentially immobilized below 630°C (the Ductile Brittle Transition Temperature, D-B-T-T). So, TiAl shows brittleness below the D-B-T-T. In Ti_3Al (DO_{19} structure), brittleness is explained by the insufficient number of slip systems. Slip is strictly limited to the basal slip (b = a/3[1120]) below 700°C [14]. Sastry *et al* concluded that Ti_3Al is brittle due to the very high degree of planarity of the slip [14].

Above the D-B-T-T, both of TiAl and Ti_3Al show ductility

because the pinning of a/6[112] is removed in TiAl while non-basal slip becomes possible in Ti_3Al.

2-2. Toughening of Aluminides

The first way to improve the toughness of aluminides is microalloying. Liu *et al* reported on a thoughened Ni_3Al alloy obtained by microalloying [15]. According to Liu *et al*, Ni-(18±2)%Al-(8±2)%Cr-(1.0±0.8)%(Zr or Hf)-(0.15±0.1)%B-<0.1wt%(C and Ce) is coldformable and possesses properties superior to Waspaloy [15]. In this alloy, boron contributes to the toughness by increasing the cohesive strength of grain boundaries, Zr or Hf contributes to high temperature strength by solid solution strenghening; Cr to high oxidation resistance; C and Ce to the adjustment of grain size. Sastry *et al* reported that Nb addition in Ti_3Al was effective in improving its ductility [14]. The effect of the Nb addition was presumed to reduce the degree of planarity of the slip.

The other way which seems attractive to improve the toughness of aluminides is fabrication of composites. While fabrication of composites was first applied for toughening of ceramics, this method has recently been widely investigated for the purpose of toughening aluminides [16][17]. Several toughening mechanisms have been proposed for fiber reinforced composites [18].

(1) Frictional load-transfer between fiber and matrix.

(2) Matrix prestressing.

(3) Crack impediment.

(4) Crack deflection.

(5) Crack branching along the fiber matrix interface (including fiber pull out).

More than one toughening mechanism is generally active, and the relative contribution of individual mechanisms depends on microstructure, fiber-matrix elastic constant and the properties of the interface. The usefulness of these mechanisms has been reported in many systems: SiC whisker reinforced Al alloys [19][20][21], graphite reinforced Al [21], and many others [22][23].

2-3. Toughening by the Dispersion of Ductile Particles

While ceramic particles, whiskers, and fibers are usually chosen as reinforcement materials [21], dispersed metallic particles are also useful as reinforcements. After the drastic change in crack propagation rate was reported in NaCl containing Ag particles [24], dispersed metallic particles in the brittle materials came to attention as reinforcements.

McHugh *et al* [25] reported that the transverse rupture strength in Al_2O_3-Mo alloy increased with increasing volume fraction of Mo and reached a maximum at 5vol% Mo. They correlated the transverse rupture strength with microstructure and considered that the strength increase was caused by the grain size refinement. The effect of Mo addition was understood to inhibit both grain growth and secondary recrystallization. Hing *et al* [26] examined MgO-Ni, MgO-Fe and MgO-Co alloys and reported that the work of fracture was higher than the effective surface energy for crack initiation by an order of magnitude in all of the three specimens. They attributed this result to the plastic deformation of the dispersed

metallic particles during the opening of the crack.

Mendelson *et al* [27] reported that both the fracture initiation energy and the fracture strength of wustite were substantially increased when a continuous α-Fe network was formed by the eutectoid reaction,

$$Fe_{0.94}O \rightarrow 0.19\ \alpha\text{-Fe} + 0.25\ Fe_2O_3 \quad \cdots\cdots (2)$$

They concluded that this phenomenon was explained by plastic blunting of the crack tip or by crack-tip pinning. Krstic *et al* [28] reported that a glass/partly oxidized Al composite showed a 60 times larger toughness than pure glass. They considered that the bulk of the energy consumed during crack propagation was expended in fracturing of Al ligaments behind the crack front.

One model to explain the effect of dispersed particles on crack propagation is the increase of a line energy of the crack front proposed by Lange [29]. In this model, the idea of line energy of a crack front is introduced and the interaction between particles and crack front is assumed. As a crack just begins to propagate within a stressed composite material, the crack front bows out between the second-phase dispersion while still remaining pinned at all the positions where it encounters the dispersion. The critical value of toughness, G_c, is expressed as

$$G_c = 2\ (\ \gamma + T/d\ ) \quad \cdots\cdots (3)$$

where γ : surface energy of the material

T : line energy of the crack front

d : spacing of dispersed particles

The second term of this expression for G_c corresponds to the increase of toughness caused by the dispersion of particles.

Although this model can explain the toughness increase in some systems, the model is very naive as Lange points out himself [29].

Evans and co-workers recently reported a numerical model study on the effect of dispersed particles from the view of a bridging zone formation [30][31]. They tried to calculate the change in the strain energy release rate, ΔG, caused by intact ligaments, directly from the J-integral around the traction zone. The critical value, ΔGc, is expressed as

$$\Delta Gc = f\int_0^{u*} \sigma(u)du \quad \cdots\cdots (4)$$

where f : volume fraction of dispersed particles

u : crack opening

σ : normal stress on the ligament

u* : crack opening when the particle fails

They solved this equation for the case of brittle materials with dispersed ductile particles under the following three asumptions.

(1) The matrix does not distort elastically.

(2) Ductile failure occures by necking to a point in a ligament.

(3) The ductile material outside the crack surfaces flows into the bridge between the crack accompanied by a rigid body displacement.

The solution is

$$\Delta Gc = \pi f \sigma_0 a_0 \epsilon_0^{-n} g(n) \quad \cdots\cdots (5)$$

$$\text{where} \quad g(n) = 2^n \int x(1-x)\ln(1/x)[-\ln(1-x)]^n dx \quad \cdots\cdots (6)$$

$$x^2 = 2\pi(u/a_0) \quad \cdots\cdots (7)$$

σ_0 : yield stress

a_0 : initial radius of the enclave

ϵ_0 : yield strain

n : hardening rate

From this equation, toughness increases in WC-Co and Al_2O_3-Al systems under given conditions were predicted [31]. The results were .

WC-Co : $\Delta G_c = 60 J/m^2$ (f=0.20, a_0=2μm, σ_0=450MPa, n=0.2)

Al_2O_3-Al: $\Delta G_c = 40 J/m^2$ (f=0.2, a_0=2μm, σ_0=70MPa, n=0.2)

However, the measured ΔG_c were much larger than the predicted values, $450 J/m^2$ in WC-Co and $180 J/m^2$ in Al_2O_3-Al [31].

Evans and co-workers considered that these discrepancies in toughness between the predicted and the measured were due to an inadequate description of the $\sigma(u)$ relationship and partly due to residual stress effects. Since the thermal expansion coefficients of metals are usually larger than those of ceramics, residual tension exists in the metal and residual compression in the ceramics. The residual stress affects the toughness because the compressive stress in the matrix must be exceeded before crack opening within the bridging zone can commence. The increment in toughness attributed to the residual stress, ΔG_R, is expressed as

$$\Delta G_R = \alpha f \sigma_R u^* \quad \cdots\cdots (8)$$

where α : a coefficient that depends on the precise nature of the $\sigma(U)$ function

σ_R : the residual stress in the metal

Considering these analyses, ductile phase reinforced aluminides seems very attractive.

In the present research, Nb_3Al was chosen as a brittle intermetallic phase and a Nb(Al) solid solution phase as a ductile

phase. One of the reasons for this selection was that this material had a possible application at elevated temperatures because both Nb_3Al and Nb possessed high melting temperatures. The other reason was that mechanical properties of Nb_3Al had not been reported yet as mentioned before. One of the aims of this research was to bring out the usefulness of Nb(Al) solid solution phase as a reinforcement. Much improvement in toughness is expected by dispersion of the ductile Nb(Al) phase in Nb_3Al matrix.

2-4. Fracture mechanics in composites

Fracture mechanics for composites is more complicated than for monolithic materials, because elastic constants of matrix, reinforcement and interface are different from one another. Tensile tests of the fiber reinforced composite show three stages [32].

(1) Initial linear load increase, corresponding to the elastic behavior of the matrix.

(2) Non-linear load increase, caused by matrix cracking and interfacial failure. In this stage, most of the load is carried by intact fibers.

(3) Load loss and failure, corresponding to the failure of fibers.

Strength of interface between matrix and fiber is an important factor. Interfaces must be sufficiently weak for substantial debonding to occur ahead of the crack.

Marshall *et al* [33] investigated SiC reinforced glass ceramic composite by using *in situ* observations during tensile and flexural loading. They reported the three stages mentioned above: an elastic

region, a non-linear deflection coinciding with the formation of matrix cracks and the final separation caused by fiber fracture and pullout.

2-5. A-15 Compounds

Nb_3Al is an intermetallic compound which has the A-15 structure. The A-15 structure is common among the superconducting materials such as Nb_3Sn, V_3Ga and V_3Si.

The mechanical properties of Nb_3Al are unknown as mentioned before. However, they can be anticipated of analogy with other A-15 materials. All intermetallics mentioned, Nb_3Sn, V_3Ga, and V_3Si, are brittle at ambient temperatures [34][35][36]. Therefore, Nb_3Al must be expected to be brittle at ambient temperatures, too. Since Nb is known to possess good ductility at ambient temperatures, Nb_3Al/Nb(Al) is a suitable material to examine the toughening mechanism of a brittle material by the dispersion of a ductile phase.

3. Experimental Procedure

3-1. Raw Materials

The raw materials used in this research were pure Al powder and pure Nb powder. Pure Al powder was obtained from Valimet Co., Ltd. It is a gas atomized, spherical powder of ±3μm in diameter. This powder was chosen because gas atomized powder was considered to contain less oxygen than powders prepared by other methods.

Pure Nb powder was available from two sources, AESAR (A powder) and Cerac (C powder). Although the average diameter was approximately 10μm in both powders with as received state, they contained coarse particles among them. So, the milling of powder C was carried out to obtain fine powder. In this research, both the as-received A powder (coarse powder) and ground C powder (fine powder) were used.

3-2. Preparation of Fine Nb Powder

Nb powder cannot be ground because it possesses ductility. However, since Nb hydride is brittle and can be ground, a hydriding-dehydriding method was used to obtain fine Nb powder.

First, Nb powder (C powder) was hydrogenated under a 100% H_2 atmosphere at 700 - 750°C and cooled down very slowly while recharging H_2 gas [37][38]. Then, the formed niobium hydride powder was ground with WC-Co balls for 6Hrs in hexane. Finally, the powder was heated up to 1200°C under vacuum. Through these processes, fine Nb powder was obtained. **Fig.1** and **Fig.2** are SEM photographs of A powder and ground C powder, respectively.

3-3. Mixing

Three types of mixed powders were prepared. Each batch had a different Nb source and a different Nb content. The Nb source and Nb content are shown in **Table 1**.

Mixing was carried out in toluene while agitating the fluid, for 20 minites. After drying, mixed powder was obtained.

3-4. Consolidation

In this research, two processes were tested to get sintered specimens. One is a "Cold Compaction and Reactive Sintering" method, and the other is a "Synthesis and Hot Pressing" method.

In the first method, mixed powder (Mixed sample, No.1) was die-pressed at the pressure of 46ksi (313MPa) - 76ksi (521MPa); then the cold compact was heated to 1200°C under He. During the sintering the following reaction takes place.

$$3Nb + Al = Nb_3Al \quad \cdots\cdots (9)$$

Since this reaction is exothermic, a large amount of heat is liberated which may assist in densifying the specimen very rapidly once the reaction takes place. However, this attempt was not successful, and only low density, inhomogeneous materials resulted.

In the second method, mixed powder (Mixed samples, No.1, No.2, and No.3) was heated up to 1200°C under He in a Al_2O_3 boat. During this process the above mentioned reaction occurred and Nb_3Al powder was obtained. Then, the synthesized powder was charged in a graphite die and hot pressed at 1600°C - 1700°C, under vacuum. The pressure applied was 5400psi (37 MPa), for 10 minites; the resultant sample size was 12.5mm diameter and 5 - 8 mm thick.

3-5. Characterization

Hot pressed samples were examined by X-ray diffraction, SEM (Scanning Electron Microscopy), EDXS (Energy Dispersive X-ray Spectroscopy) and micro indentation (1Kg Load). Samples were prepared by mechanical polishing followed by chemical etching in a $HF-HNO_3$ aqueous solution. The same characterization was carried out after the specimens were heattreated at 1700 - 1800°C. The purpose of the heat treatments was to vary the volume fraction of Nb phase through precipitation.

4. Results

4-1. Cold Compaction and Reactive Sintering

Fig.3 shows densities of the specimens before and after sintering as a function of compaction pressure. The density dropped due to the sample swelling during sintering. **Fig.4** shows a SEM micrograph of a polished surface. Fig.4 suggests the existence of a liquid Al phase between the Nb particles during sintering.

It is reported that liquid phase sintering causes sample swelling during sintering unless several criteria are satisfied [31]. So, this result is understandable. This problem will be discussed in the discussion section. After this, the cold compaction and reactive sintering method was abandoned, and all the data in this report are the ones obtained by the synthesis and hot pressing method.

4-2. Synthesis

Synthesized powders were examined by X-ray diffraction and SEM. **Fig.5** - **Fig.7** show the X-ray diffraction patterns of the synthesized powders (Mixed samples, No.1, No.2 and No.3). Many peaks in **Fig.5** represent Nb_2Al phase which has a complicated FeCr (σ) structure. Many peaks are superimposed on other peaks of Nb_2Al, Nb_3Al and Nb. For example, the main peak observed at 2θ=38.7° is a superimposed peak of (330)Nb_2Al, (210)Nb_3Al and (110)Nb. So, attention must be paid to a special peak which is not superimposed on other peaks, to identify the phases. Identifying Nb_2Al is relatively easy because it has several strong peaks which do not

overlap other peaks, eg. (410)(2θ=37.3°), (212)(2θ=40.4°), (411)(2θ=41.3°) etc. To identify Nb_3Al and Nb, (320)Nb_3Al (2θ=64.7°) and (112)Nb (2θ=69.8°) were checked because they are the only ones not superimposed by others. Near (320)Nb_3Al and (112)Nb, there is a Nb_2Al peak which does not have superposition, ie. (532)Nb_2Al (2θ=65.6°). So, 2θ range of 2θ = 61° - 71° was minutely examined for the purpose of phase identification.

From the results, the phases each specimen contains are as follows:

The specimen 1 : Nb_2Al, Nb_3Al and Nb

The Specimen 2 : weak Nb_2Al, Nb_3Al and Nb

The specimen 3 : Nb_3Al and Nb

Since the Nb_2Al phase reflection is weak in **Fig.6** and is not detected at all in **Fig.7**, the Nb_2Al phase is considered to be resulted from coarse Nb particles. If the system corresponds to the equilibrium phase diagram correctly, only the Nb_3Al exists at 1200°C in 93wt% Nb alloy and two phases of Nb_3Al and Nb exist in 94wt% Nb alloy (**Fig.8**) [40]. So, these results show that if the specimen contains coarse Nb particles, Nb remains unreacted and the actual composition shifts to the Al-rich side. This problem of composition shift can be removed by avoiding coarse Nb powder.

Fig.9 shows SEM micrograph of synthesized powder, No.2.

4-3. Hot Pressing

Hot pressing could be completed successfully. There was no reaction between the synthesized powder and the graphite die, was there no evapolation loss under high vacuum (10^{-5} mmHg).

Densities of the specimens after hot pressing were shown in **Table 2** as well as the process variables. Theoretical densities (7.51g/cm3 for 93 wt% Nb, 7.65g/cm3 for 94 wt% Nb) were calculated on the assumption that stoichiometric Nb_3Al (ρ=7.28g/cm3) and pure Nb (ρ=8.57g/cm3) occupy the same volume in the composites as they exist solely at the fraction of 93wt% Nb and 94wt% Nb, respectively. Though the density obtained at 1600°C was low, higher densities than 97% of theoretical were obtained by hot pressing above 1650°C.

Fig.10 - **Fig.12** were obtained from the specimen 1 which started from the coarse Nb powder. It is found from **Fig.10** that the specimen contains three regions, black matrix(A), white region(B) and black round region(C) surrounded by white region. EDXS analyses (**Fig.11**) show that Nb and Al are detected in both the region (A) and the region (B), and only Nb is detected from the (C). From the X-ray diffraction patterns of this specimen (**Fig.12**), it is found that Nb_3Al and Nb exist in the specimen. Therefore, it is concluded that the (A) is Nb_3Al phase and the (C) is pure Nb and the (B) is a transition area caused by coarse Nb particles. The phase (B) is considered to have the Nb structure for the following two reasons. 1) The solid solubility of Al in the Nb is about 5 wt% at 1700°C, and 2) all of the Nb peaks in Fig.12 slightly shift in the larger direction of 2 theta. A typical peak shift is shown in Fig.12(b). So, the region (B) is concluded to be a Nb solid solution phase which contains Al close to the solubility limit. This phase is expressed as Nb(Al) in this report.

Similar results were obtained from the specimen 2. Corresponding to the fine Nb powder used as a starting material, no

"pure" Nb phase like in Fig.10 was observed by SEM (SEM micrograph is shown in **Fig.22**). Although no other peak was detected except Nb_3Al and Nb by X-ray diffraction in this specimen (**Fig.13**), black particles were observed, and Al and weak Nb signals were detected in these particles (**Fig.14**). These black particles are considered to be aluminum oxide, but their exact composition is still unknown.

Fig.15 - Fig.17 are obtained from the specimen 3 which has 94wt% Nb content. As shown in **Fig.15**, this specimen shows quite different microstructure from the specimens of 93wt% Nb. There is no "distributed" Nb(Al) phase. Matrices and grain boundary-like thin layers are observed as well as small particles. And the morphological variety is also observed in matrices. Some are relatively small and have a smooth periphery like (A) in Fig.15(b). Some are relatively large and have uneven periphery like (B). However, there was no significant difference in EDXS analysis between these two types of matrices (Fig.16(a) and (b)).

Nb and Al were detected in the thin layer (C) and strong Al and weak Nb signals were obtained from the small round particles (D) (**Fig.16**). From the X-ray diffraction analysis (**Fig.17**), it is found that this specimen contains only Nb_3Al and Nb. And the shift of Nb peaks to higher 2θ direction is the same as other two specimens. Of course the intensity of Nb peaks was higher than those in other two specimens. Therefore, it is concluded that the matrix (A) and (B) are Nb_3Al, and grain boundary-like layer (C) is Nb(Al) solid solution phase. The exact composition of the region (D) remains unknown.

Fig.18 shows the micrographs of the specimen 1, heat-treated at 1800°C. The lamellar phases (A) are determined to be precipitated Nb phases (**Fig.19**). The heat treatment was carried out at three temperatures, 1700°C, 1750°C and 1800°C. The precipitation of Nb phase is common at three temperatures. And there was no significant difference among the heat treatment temperatures. Micrographs of heat treated specimens, 2 and 3, are shown in **Fig.23** and **Fig.24(b)**. From Fig.24(b), it is found that the grain boundary-like Nb(Al) phase turned into the lamellar Nb(Al) phase during heat treatment.

4-4. Toughness

Fig.20 shows the indentation test results of the specimen 1. In the hot pressed specimen, cracks are observed starting at the edge or the corner of the indenter. When the crack meets with the Nb phase, it is pinned by the Nb phase (A) or propagates forward without penetrating the Nb phase (B). This results in the reduction of the crack length in both cases.

Cracks are also observed in the heat treated specimen (**Fig.21**). However, the number of cracks nucleated from the indenter is smaller than in the hot pressed specimen, and some corners and edges do not have any crack. For example, no crack is observed at the indenter corner (A), and the edge (A) - (B). In this case, the corner (A) is touching the Nb phase. On the other hand, crack propagation is observed near the corner (B). In a high magnification figure (**Fig.21(b)**), it is found that this crack cannot penetrate the Nb phase (C), and is finally pinned by

the Nb phase (D). Qualitatively speaking, the inhibition of crack propagation is more effective in the heat treated specimen than in the hot pressed specimen. The total crack length becomes shorter and the number of corners and edges which have no crack increases. It should be noted that the hardness decrease of the specimen after the heat treatment is not large ($\Delta Hv=40$).

Almost the same results were obtained from the specimen 2 (**Fig.22**, and **Fig.23**). In this specimen, heat treatment was also effective. The crack was suppressed more effectively after heat treatment, and hardness decrease was almost zero.

In the specimen 3 which has higher Nb content (94wt% Nb), differrent results were obtained. No crack was observed at all in the hot pressed specimen (**Fig.24(a)**). However, crack initiation was observed and hardness value increased after heat treatment (**Fig.24(b)**). As described previously, the grain boundary-like Nb(Al) phase disappeared and the lamellar Nb(Al) phase precipitated during heat treatment. Crack initiation in the heat-treated specimen may by attributed to the change of Nb phase morphology which is considered to be accompanied with the change in interfacial strength. This will be discussed in the discussion section. At least it is clear that a grain boundary-like Nb(Al) phase is more effective as an obstacle to crack initiation than the lamellar precipitated Nb(Al) phase.

5. Discussion

5-1 Processing

The main results obtained on processing are as follows:

(1) The preparation of highly densified Nb_3Al/Nb composite material was possible by the method of Nb_3Al synthesis and hot pressing.

(2) The specimen expanded during sintering when the cold compaction and reactive sintering method was used.

(3) The particle size of Nb powder was the important factor which influenced the phase distribution and phase content of the specimen. To obtain the exact phases expected from the equilibrium phase diagram, the preparation and use of fine Nb powder was essential.

(4) An unknown phase was observed in the hot pressed specimens.

First, the result (1) is discussed. The establishment of the fabrication condition is important. The optimum conditions are tabulated in **Table 3**. Although the synthesis and hot pressing method is not new in itself, it represents the first application to the fabrication of Nb_3Al/Nb composite material.

Next, the result (2) is discussed. According to German [39], the initial stage of the liquid phase sintering is influenced by many factors, and the specimen swells if these factors are unfavorable. The factors are

Solubility ratio

Diffusivity ratio

Particle size

Green density

Contact angle

Dihedral angle

Temperature

Time.

Among them, the solubility ratio is the most important factor which dominates the mass transfer. Here the solubility ratio is defined as the solubility of the base metal (Nb) in the liquid of the additive (Al) devided by the solubility of the additive in the base metal. At the eutectic temperature solubility of Nb in Al is less than 0.3at%, and the solubility of Al in Nb is 8 at%. So the solubility ratio is less than 0.0375. In such a situation, liquid Al is prone to melt into Nb particle and Nb is not prone to melt into the Al liquid phase. So, one-way mass transfer occurs and this results in pore formation at the Al position and in expansion at the Nb position. Since the solubility ratio is not changeable, this system can be said to be an intrinsically swelling system. However, German *et al* reported that they obtained densified material (95% of the theoretical density) by applying a cold compaction and reactive sintering method in this system [41]. This fact may mean that the densification is possible even in the unfavorable systems if other factors (changable process variables) work favorably. The surface state of the powder (thickness of oxide layer), particle size, heating rate and green density might be the important factors which dominate the process. The effect of these process variables was not made clear in this research. The reactive sintering is still more of an art.

The result (3) is very reasonable. Since the distribution of

Nb phase is the most important factor which dominates the cracking behavior in this material, the starting Nb powder should be fine to obtain a uniform Nb distribution as well as to realize the equilibrium state.

The result (4) remains still unknown. From the X-ray diffraction, only Nb and Nb_3Al peaks were detected. By EDXS analysis, Al was detected in these particles. Therefore, one possible explanation is that these particles are aluminum oxides and that they can not be detected by X-ray diffraction because their intensity is below the sensitivity level of the detection. If this is true, new questions emerge: When were these particles formed? How can these particles be avoided? These questions need further work to be solved. Possibly, oxygen contamination in the powder can lead to the formation of Al_2O_3 when powders are processed.

5-2. Evaluation of Toughness

This research has shown that the Nb(Al) phase acts as an obstacle to both crack initiation and crack propagation. This effect is more pronounced with increasing Nb(Al) phase content. The precipitation of Nb(Al) phases is effective in toughening the 93wt% Nb specimen. Also, there is a difference in the effect of the lamellar precipitated Nb(Al) phase compared to the grain boundary-like Nb(Al) phase in the higher Nb content material. The latter appears more effective as an obstacle to crack initiation. The network of the Nb(Al) phase established by grain boundary-like Nb(Al) phases is considered to play a dominant role in crack inhibition. This consideration is supported by the decrease in

crack inhibition after a heat treatment that leads to the disappearance of Nb(Al) phase network. The reason of this difference for the two Nb(Al) phase morphologies is not clear. Factors influencing the toughness are σ_0, a_0, ϵ_0 and n from the equation (5). And the interfacial strength between the matrix and the Nb(Al) phase is also influencing toughness. It is clear that the Nb(Al) phase changed its morphology from a grain boundary-like one to a lamellar one during heat treatment. However, it is not clear how the above mentioned five factors changed during heat treatment. It is not reasonable to expect a drastic change in σ_0, ϵ_0 and n because the crystal structure and the composition of Nb(Al) phase itself can be considered not to have changed significantly. Also, a_0 is almost the same in the two different morphologies of the Nb(Al) phases. So, the change in interfacial strength may be considered to be responsible for the decrease in toughness, although no direct evidence has been obtained to date. If this is true, the observed decrease in toughness can also be explained by the bridging zone model, but this interpretation needs further work to be verified.

Quantitative data on toughness could not be obtained in this research because the cracking patterns differed for the different indentations (in the same specimen). This may be explained by different Nb(Al) phase distribution on a local scale, so that the cracking pattern is very sensitive to the distribution of Nb(Al) phases.

Indentation is a very convenient method for quick evaluation of toughness. However, some requirements must be fulfilled for

indentations to correlate well with toughness. First, the effect of the residual stress on the surface must be removed [42][43]. In this research, all of the specimens were chemically etched before indentation. Although the thickness of removed surface layer was not measured, the damaged layer was considered to be removed by chemical etching. Next, the indenter size must be at least ten times larger than grain size to avoid the effect of microstructural non-uniformity [35]. This requirement could not be satisfied in this research. The indenter size was not large enough compared to the spacing of Nb(Al) phase. So, cracking patterns were different for each indent and even for each corner of the same indent. Also, cracks nucleated at the sides of the indenter instead of at the corner. It is evident that stress intensification was changed by the presence of Nb(Al) phase.

Testing of compact fracture specimen will be required to determine the toughness quantitatively. A suitable sample size for the deflection test is a disk of 1 1/2 inch ϕ . Hot pressing of 1 1/2 inch ϕ specimen can be carried out by applying the same condition described in Table 3.

6. Conclusion

Nb_3Al/Nb composite materials were fabricated by a powder metallurgical technique, and the effect of Nb phase on the toughness of this material was examined. The following interesting results were obtained.

(1) Highly densified Nb_3Al/Nb was successfully produced by Nb_3Al powder synthesis and hot pressing. The process variables suitable for the production of this material have been determined.

(2) Cracking in the $Nb_3Al/Nb(Al)$ was strongly influenced by the presence of Nb(Al) phases. Some examples of crack propagation without penetrating the Nb phase and crack pinning were shown. And the total length and number of the cracks decreased with increasing Nb phase content. Further, the grain boundary-like Nb phase was more effective as an obstacle to crack than the precipitated lamellar Nb phase. These experimental results present very good qualitative agreement with the toughening mechanism by bridging zone formation.

References

[1] K. Aoki and O. Izumi, *Journal of Japan Institute of Metals*, Vol.43 (1979) P.1190.

[2] J.B. AcAndrew and H.D. Kessler, "Ti-36 Pct Al as a Base for High Temperature Alloys", *Journal of Metals*, October (1956) P.1348-1353.

[3] H.R. Ogden, D.J. Maykuth, W.L. Finlay, and R.I. Jaffee, "Mechanical Properties of High Purity Ti-Al Alloys", *Journal of Metals*, Vol.5,No.2 (1953) P.267-272.

[4] J.H. Westbrook, "Mechanical Properties of Intermetallic Compounds", John Wiley & Son, (1960).

[5] E.M. Schulson, "Structure, Properties and Potential of Intermetallic Compounds Produced from Powders", *The International Journal of Powder Metallurgy*, Vol.23, No.1 (1987) P.25-32.

[6] T. Takasugi, E.P. George, D.P.Pope and O. Izumi, "Intergranular Fracture and Grain Boundary Chemistry of Ni_3Al and Ni_3Si", *Scripta Metallurgica*, Vol.19, No.4 (1985) P.551-556.

[7] T. Ogura, S. Hanada, T. Masumoto and O. Izumi, "Grain Boundary Fracture of $L1_2$ Type Intermetallic Compound Ni_3Al" *Metallurgical Transactions A*, Vol.16A, No.3 (1984) P.441-443.

[8] C.T. Liu, C.L. White and J.A. Horton, "Effect of Boron on Grain Boundaries in Ni_3Al", *Acta Metallurgica*, Vol.33, No.2 (1985) P213-229.

[9] T. Takasugi and O. Izumi, "Electronic and Structural Studies of Grain Boundary Strength and Fracture in $L1_2$ ordered alloys - 1. On Binary A_3B Alloys", *Acta Metallurgica*, Vol.33, No.7 (1985) P.1247-1258.

[10] T. Takasugi, O. Izumi and N. Masohashi, "Electronic and Structural Studies of Grain Boundary Strength and Fracture in $L1_2$ Ordered Alloys - 2. On the effect of Third Elements in Ni_3Al Alloys", *Acta Metallurgica* , Vol.33, No.7 (1985) P.1259-1269.

[11] T. Takasugi, N. Masahashi and O. Izumi, "Electronic and Structural Studies of Grain Boundary Strength and Fracture in $L1_2$ Ordered Alloys - 3. On the Effect of Stoichiometry", *Acta Metallurgica*, Vol.35, No.2 (1987) P.381-391.

[12] H.A. Lipsitt, D. Shechtman and R.E. Schafrik, "The Deformation and Fracture of TiAl at Elevated Temperatures", *Metallurgical Transactions A*, Vol.6A, No.12 (1975) P.1991-1996.

[13] T. Kawabata, Y. Takezono, T. Kanai and O. Izumi, "Bend Tests and Fracture Mechanism of TiAl Single Crystals at 293-1073K", *Acta Metallurgica*, Vol.36, No.4 (1988) P.p63-975.

[14] S.M.L. Sastry and H.A. Lipsitt, "Ordering Transformations and Mechanical Properties of Ti_3Al and Ti_3Al-Nb Alloys", *Metallurgical Transactions A*, Vol.8A, No.10 (1976), P.1543-1552.

[15] C.T. Liu and V.K. Sikka, "Nickel Aluminides for Structural Use", *Journal of Metals*, May (1986) P.19-21.

[16] G.R. Odette, H.E. Deve, C.K. Elliot, A. Hasegawa and G.E. Lucas, "The Influence of the Reaction Layer Structure and Properties on Ductile Phase Toughening in Titanium Aluminide-Niobium Composites", in "Interfaces in Metal-Ceramics Composites", P.443-463. edited by R.Y. Lin, R.J. Arsenault, G.P. Martins and S.G. Fishman, TMS (1990).

[17] A.K. Misra, "Thermodynamic Analysis of Chemical Interactions between Reinforcement Materials and Matrices in Aluminide-Based High Temperature Intermetallic Matrix Composites", in "Interfaces in Metal-Ceramics Composites", P.85-102. edited by R.Y. Lin, R.J. Arsenault, G.P. Martins and S.G. Fishman, TMS (1990).

[18] J.A. Cornie, Y.M. Chiang,D.R. Uhlmann, A. Mortensen and J.M. Collins, "Processing of Metal and Ceramic Matrix Composites", *Ceramic Bulletin*, Vol.65, No.2 (1986) P.293-304.

[19] A.P. Divecha, S.G. Fishman and S.D. Karmarkar, "Silicon Carbide Reinforced Aluminum - A Formable Composite", *Journal of Metals*, Vol.33, No.9 (1981) P.12-17.

[20] C. Milliere and M. Suery, "Fabrication and Properties of Metal Matrix Composites Based on SiC Fiber Reinforced Aluminium Alloys", *Materials Science and Technology*, Vol.4, No.1 (1988) P.41-51.

[21] C.F. Lewis, "The Exciting Promise of Metal-Matrix Composites", *Materials Engineering*, Vol.103, No.5 (1986) P.33-37.

[22] T.W. Chou, A. Kelly and A. Okura, "Fibre-Reinforced Metal-Matrix Composites", *Composites*, Vol.16, No.3 (1985) P.187-206.

[23] For example, J.R. Stephens, "Intermetallic and Ceramic Matrix Composites for 815-1370°C (1500°F to 2500°F) Gas Turbine Engine Applications", in "Metal & Ceramic Matrix Composites : Processing, Modeling & Mechanical Behavior", P.3-11. edited by R B. Bhagat, A.H. Clauer, P. Kumar anf A.M. Ritter, TMS (1990).

[24] C.T. Forwood and A.J. Forty, "The interaction of Cleavage Cracks with Inhomogeneities in Sodium Chloride Crystals", *Philosophical Magazine*, Vol.11,No.113 (8 series) (1965) P.1067-1082.

[25] C.O. McHugh, T.J. Whalen and M. Humenik,Jr., "Dispersion-Strength Aluminum Oxide", *Journal of the American Ceramic Society*, Vol.49,No.9 (1966) P.486-491.

[26] P. Hing and G.W. Groves, "The STrength and Fracture Toughness of Polycrystalline Magnesium Oxide Containing Metallic Particles and Fibers", *Journal of Materials Science*, Vol.7,No.4 (1972) P.427-434.

[27] M.I. Mendelson and M.E. Fine, "Enhancement of Fracture Properties of Wustite by Precipitation", *Journal of the American Ceramic Society*, Vol.57,No.4 (1974) P.154-159.

[28] V.V. Krstic and P.S. Nichoson, "Toughening of Glasses by Metallic Particles", *Journal of the American Ceramic Society,* Vol.64,No.9 (1981) P.499-504.

[29] F.F. Lange, "The Interaction of a Crack Front with a Second-Phase Dispersion", *Philosophical Magazine*, Vol.22, 8 Series (1970) P.983-992.

[30] A.G. Evans and R.M. McMeeking, "On the Toughening of Ceramics by Strong Reinforcements", *Acta Metallurgica*, Vol.34,No.12 (1986) P.2435-2441.

[31] L.S. Sigl, P.A. Mataga, B.J. Dalgleish, R.M. McMeeking and A.G. Evans, "On the Toughness of Brittle Materials Reinforced with a Ductile Phase", *Acta Metallurgica*, Vol.36, No.4 (1988) P.945-953.

[32] S.G. Fishman, "Ramification of Recent Microchemical Innovations on Understanding in Composite Interfaces", in "Interfaces in Metal-Ceramics Composites", P.3-29. edited by R.Y. Lin, R.J. Arsenault, G.P. Martins and S.G. Fishman, TMS (1990).

[33] D.B. Marshall and A.G. Evans, "Failure Mechanisms in Ceramic-Fiber/Ceramic-Matrix Composites", *Journal of the American Ceramic Society*, Vol.68, No.5 (1985) P.225-304.

[34] G.B. Soscia and R.N. Wright, "High Temperature Plastic Deformation of Two V-Ga Alloys with A15 Structure", *Metallurgical Transactions A*, Vol.17A, No.3 (1986) P.519-525.

[35] L.R. Eisenstatt and R.N. Wright, "Plastic Deformation in Polycrystalline Nb_3Sn". *Matallurgical Transactions A*, Vol.11A, No.7 (1980) P.1131-1138.

[36] R.N. Wright, "The Deformation of A15 Compounds", *Metallurgical Transactions A*, Vol.8A, No.12 (1977) P.2024-2025.

[37] E.A. Gulbransen and K.F. Andrew, "Reaction of Columbium and Tantalum with O_2, N_2 and H_2", *Transactions AIME*, Vol.188, March (1950) P.586-599.

[38] M.Hansen, "Constitution of Binary Alloys", P.786-788. McGraw-Hill Book Company, Inc. New York (1958).

[39] R.M. German, "Liquid Phase Sintering", Chapter 4, P.65-99. Plenum Press, New York (1985).

[40] Shunk, "Constitution of Binary Alloys, Second Supplement", P.18-20. McGraw-Hill Book Company, Inc. New York (1969).

[41] R.M. German, A. Bose and N.S. Stoloff, "Powder Processing of High Temperature Aluminides", in "High-Temperature Ordered Intermetallic Alloys 3", P.403-414. edited by C.T. Liu, A.I. Taub, N.S. Stoloff and C.C. Koch, Materials Research Society, Pittsburgh (1989).

[42] A.G. Evans and E.A. Charles, "Fracture Toughness Determination by Indentation", *Journal of the American Ceramic Society*, Vol.59, No.7-8 (1976) P.371-372.

[43] M. Shiwa and T. Kishi, "Fracture Toughness of Ceramics", *Bulletin of the Japan Institute of Metals*, Vol.27, No.8 (1988) P.644-649.

Table 1 Three types of the mixed powder

No.	Nb source	Nb content
Mixed No.1	As received A powder (Coarse)	93 wt% Nb
Mixed No.2	Ground C powder (Fine)	93 wt% Nb
Mixed No.3	Ground C powder (Fine)	94 wt% Nb

note : A powder : AESAR
C powder : Cerac

Table 2 Results of hot pressing. Applied stress (5400psi) and stress applied time (10 min) are same in all the specimens. Theoretical densities are 7.51g/cm3 for 93 wt% Nb and 7.65g/cm3 for 94 wt% Nb.

Specimen No.	Mixed No.	Temperature	Density
1-1	1	1600°C	7.08 g/cm3, 94.3%
1-2	1	1650°C	7.30 g/cm3, 97.2%
1-3	1	1700°C	7.45 g/cm3, 99.2%
2	2	1650°C	7.32 g/cm3, 97.5%
3	3	1650°C	7.45 g/cm3, 97.4%

Table 3 Tabulation of the optimun conditions in fabricating Nb_3Al/Nb composite material

Process	Condition
Raw material	
Nb powder	Fine powder, less than 1 μm
Al powder	Spherical gas atomized powder of 3 μm was used in this research
Synthesis	1200°C, under He
Hot pressing	1650 - 1700°C 5400 psi 10 min under vacuum (10^{-5} mmHg)

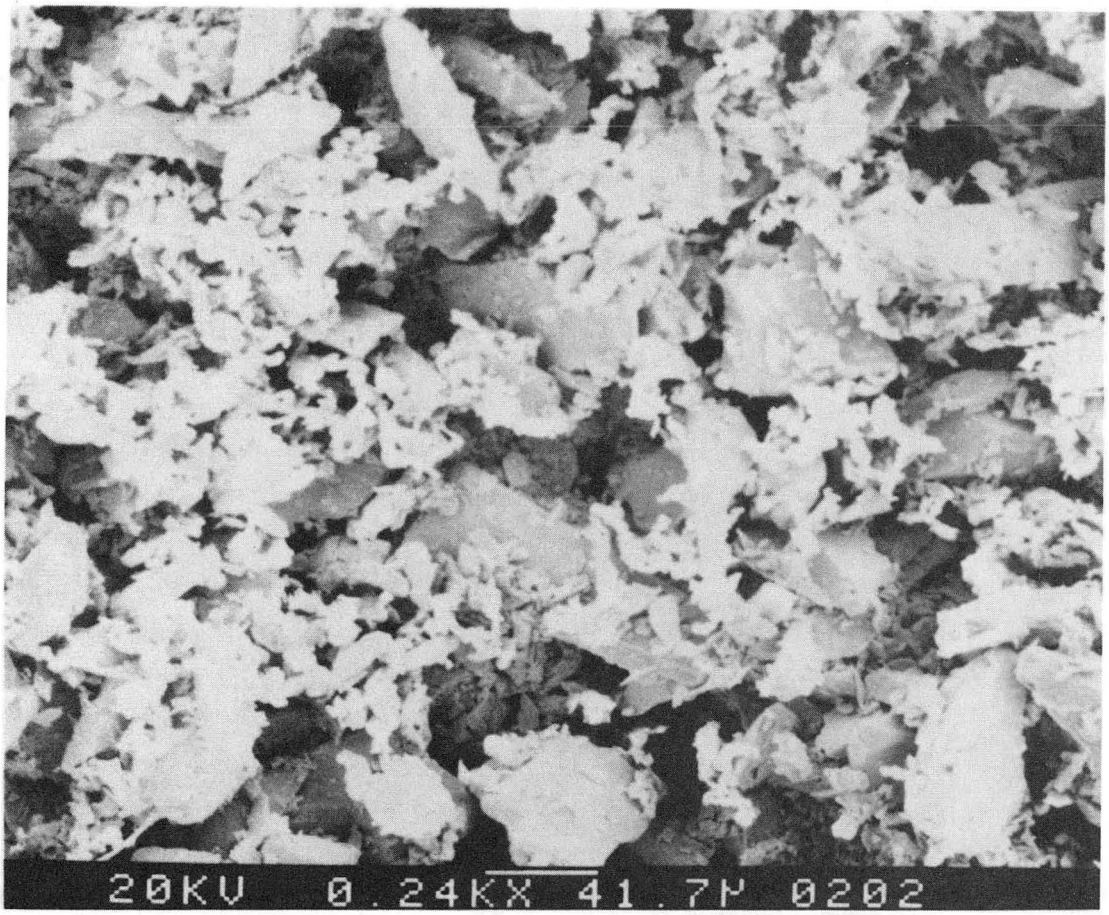

XBB 905-3685

Fig.1 SEM micrograph of the coarse Nb powder (A powder).

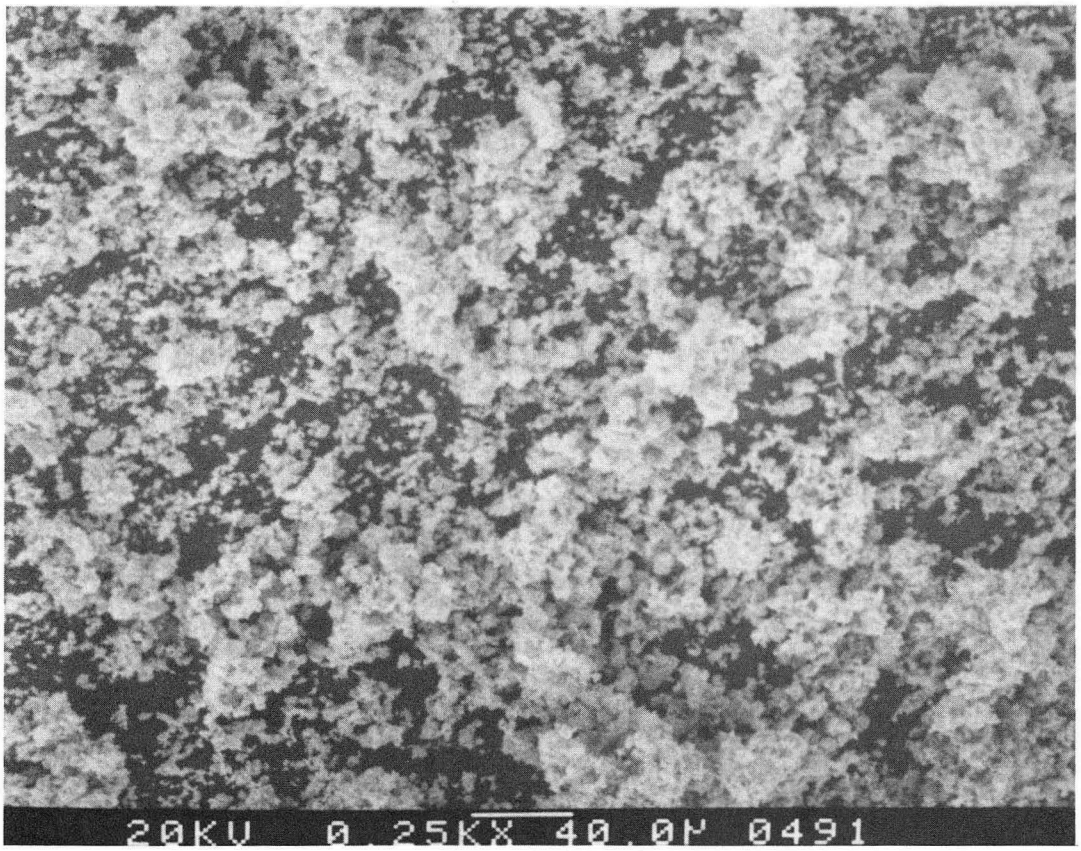

XBB 905-3684

Fig.2 SEM micrograph of the fine Nb powder (C powder).
The powder was obtained by hydriding-dehydriding method.
Milling time was 6Hrs.

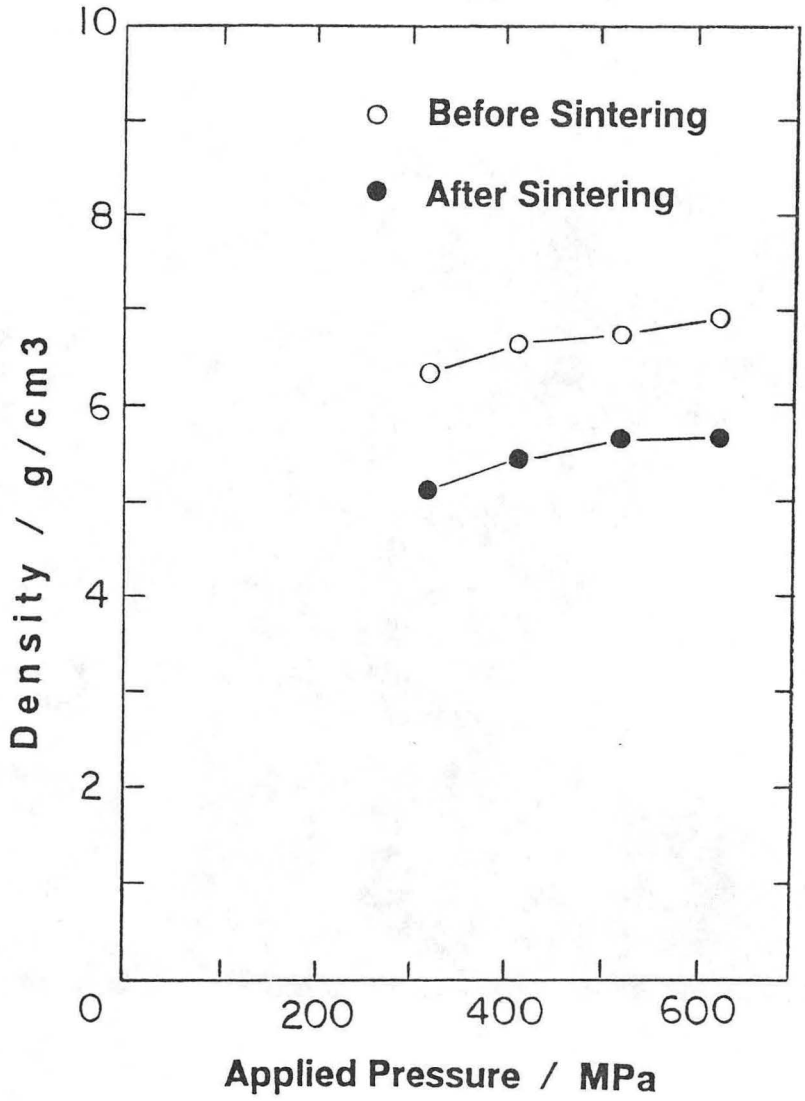

Fig.3 The results obtained by the cold compaction and reactive sintering method. The density drop is caused by the swelling of the samples during sintering.

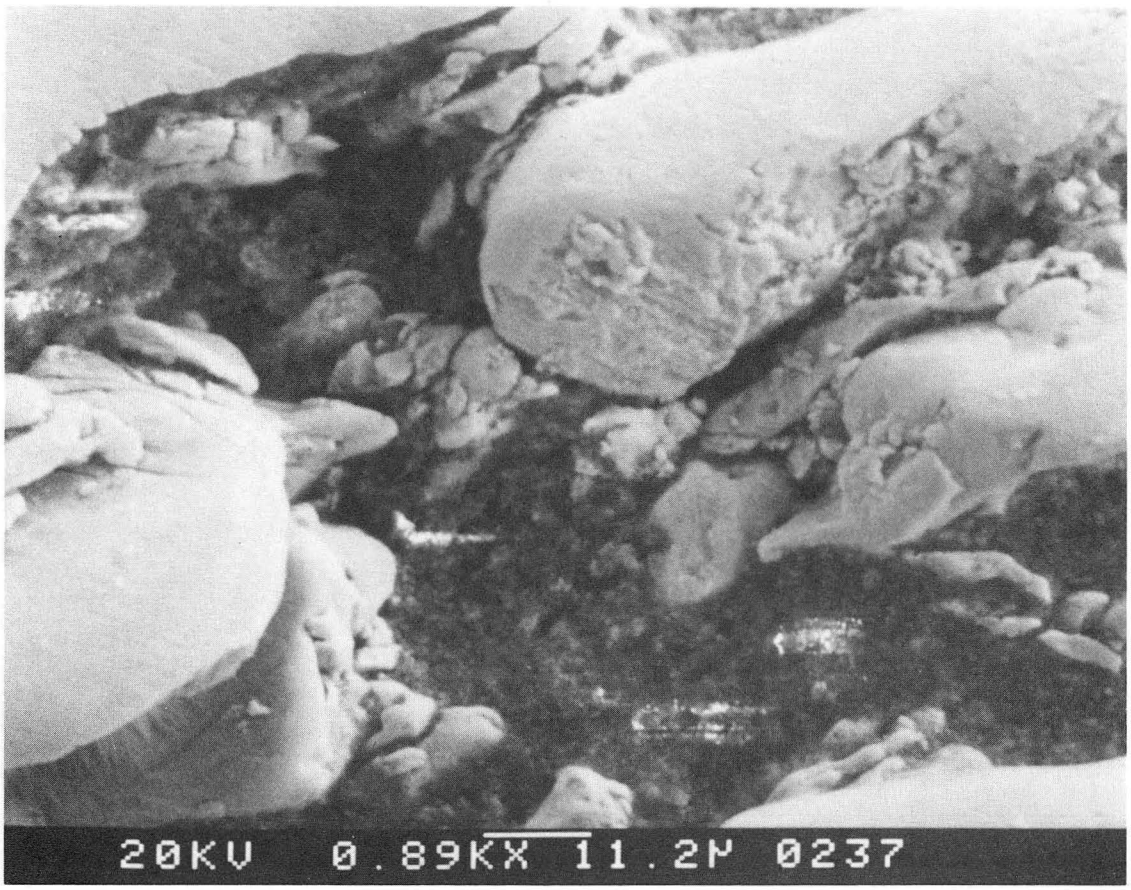

XBB 905-3683

Fig.4 SEM micrograph of the specimen obtained by the cold compaction and reactive sintering method.

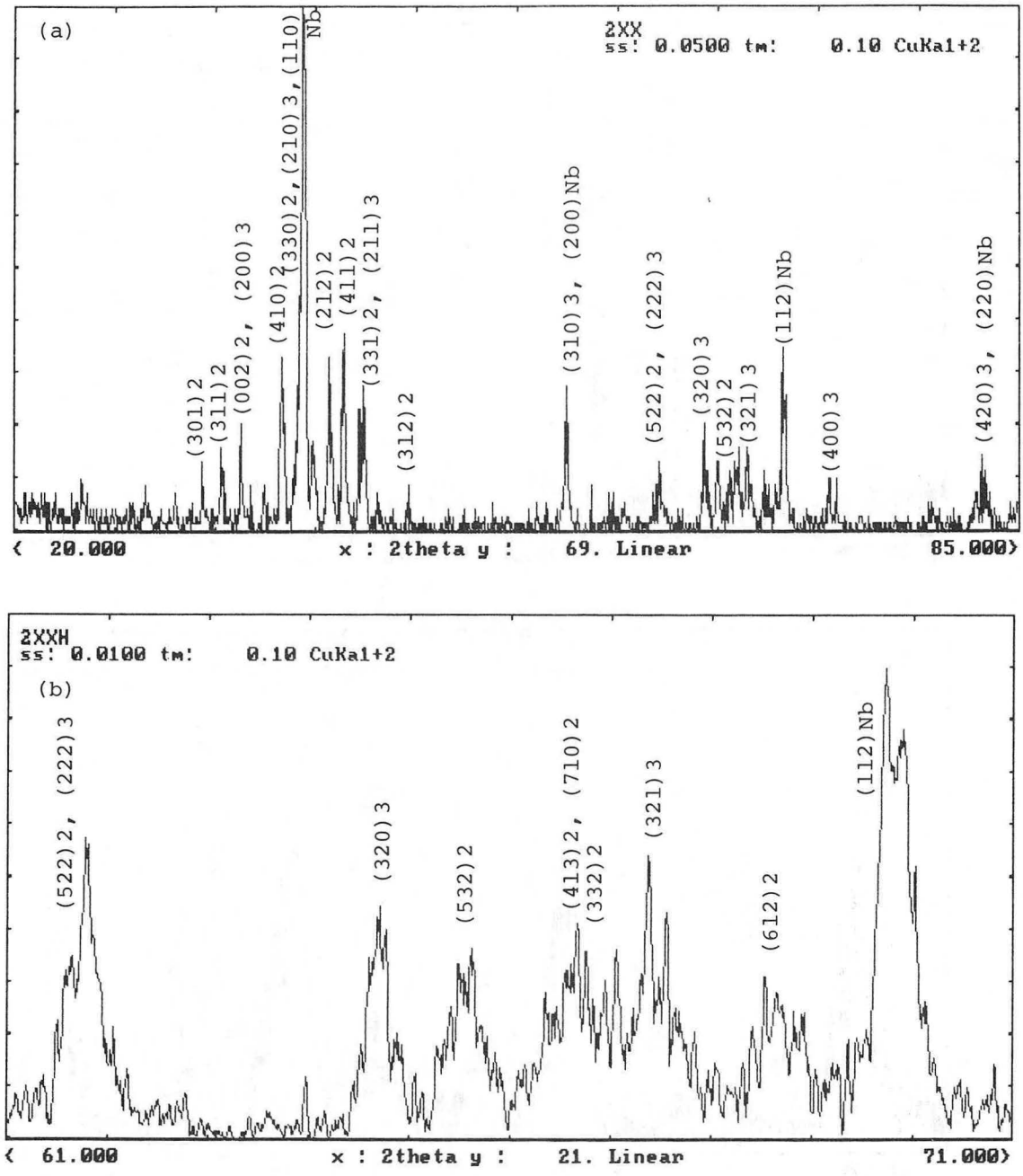

XBL 905-1707

Fig.5 X-ray diffraction patterns of the synthesized powder.
The mixed sample No.1 (Coarse powder, 93wt% Nb) was used.
(a) 2θ range : 20 - 85°
(b) 2θ range : 61 - 71°
The suffixes, 2 and 3 represent Nb_2Al and Nb_3Al, respectively.

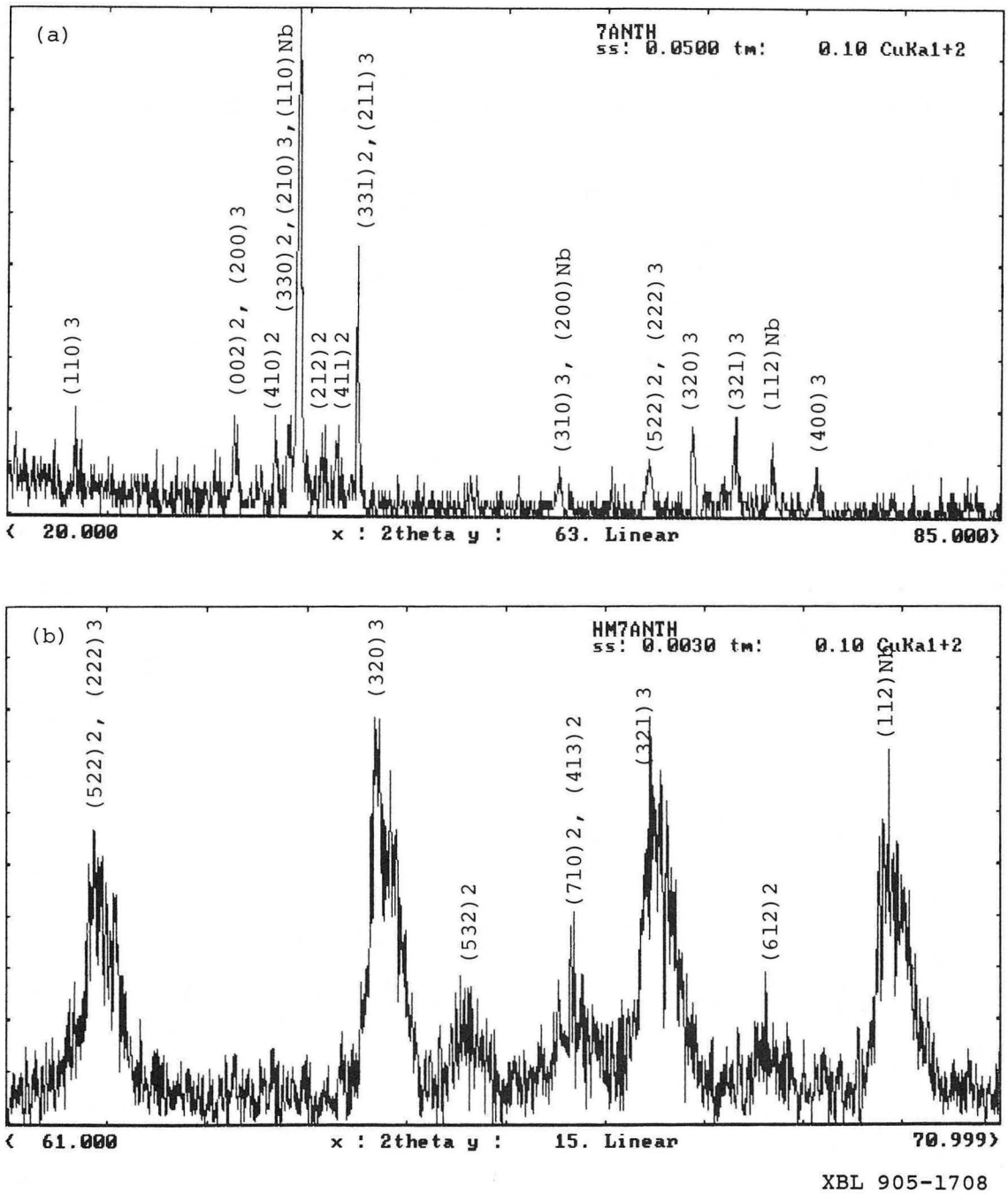

Fig.6 X-ray diffraction patterns of the synthesized powder.
The mixed sample No.2 (Fine powder, 93wt% Nb) was used.
(a) 2θ range : 20 - 85°
(b) 2θ range : 61 - 71°

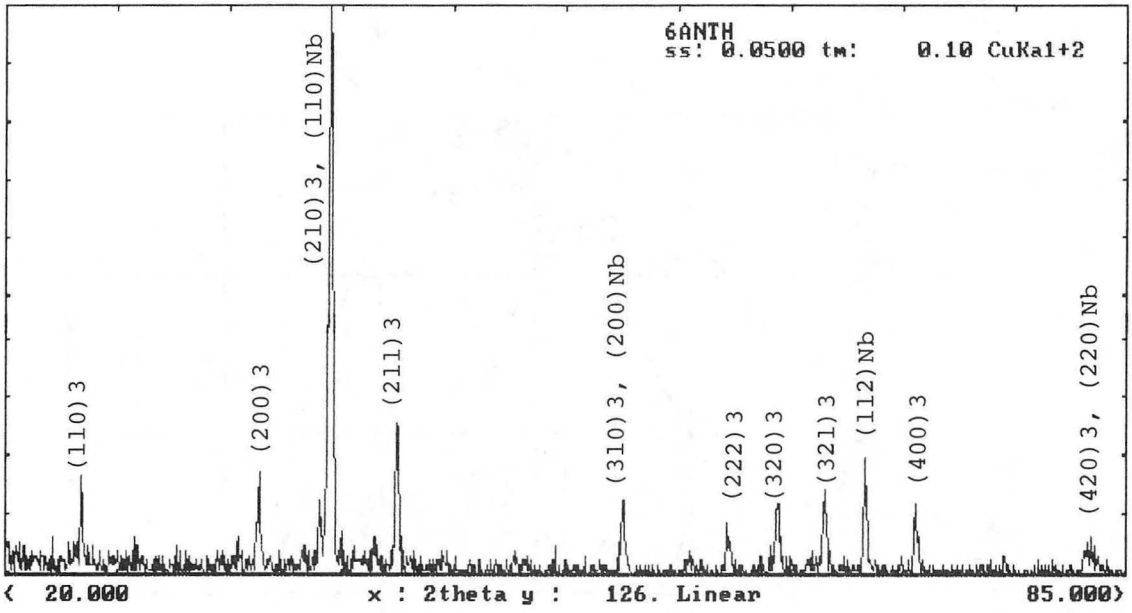

XBL 905-1709

Fig.7 X-ray diffraction pattern of the synthesized powder. The mixed sample No.3 (Fine powder, 94wt% Nb) was used.

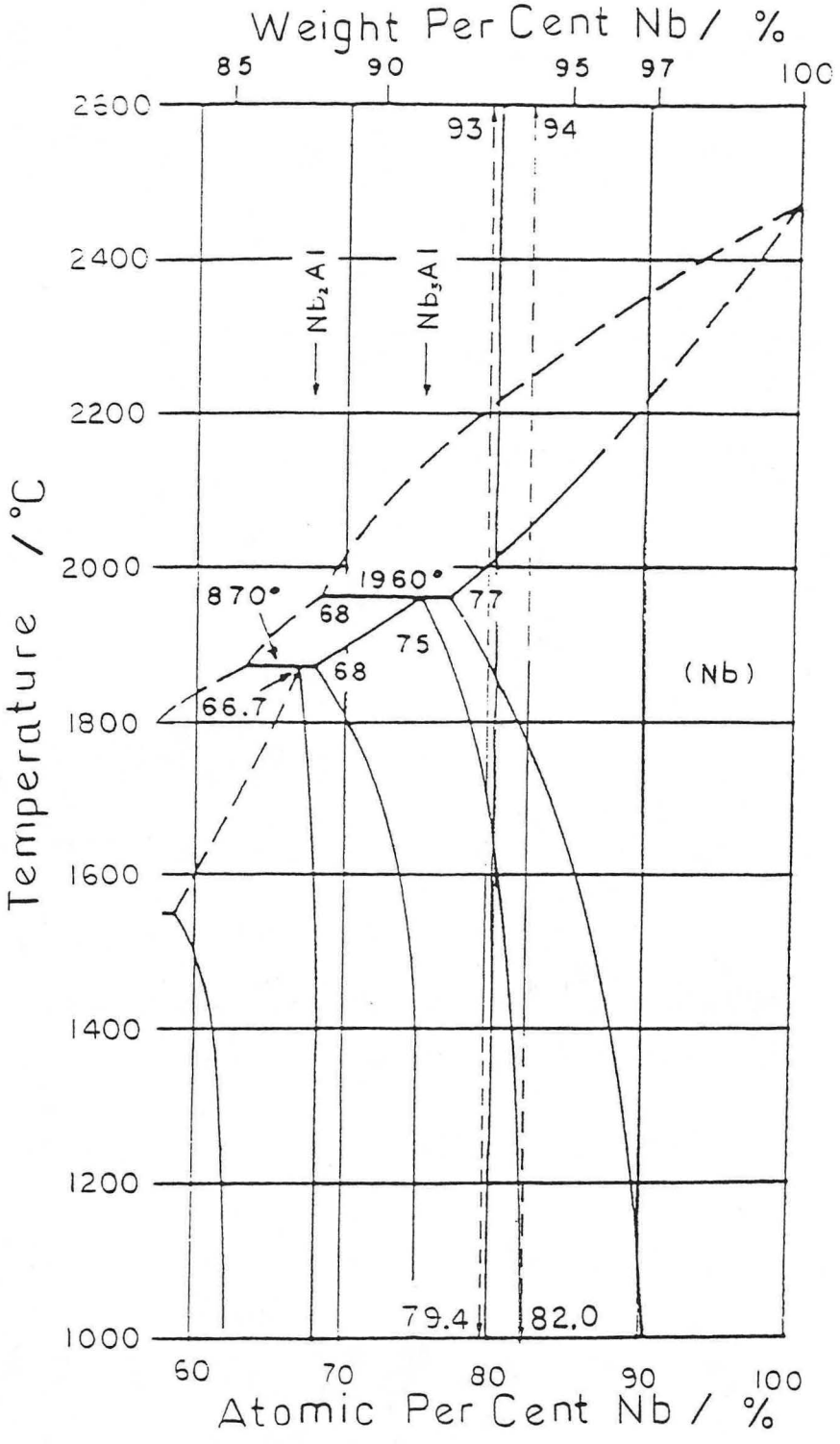

Fig.8 Phase diagram of the Nb-Al system, magnified at the Nb corner.

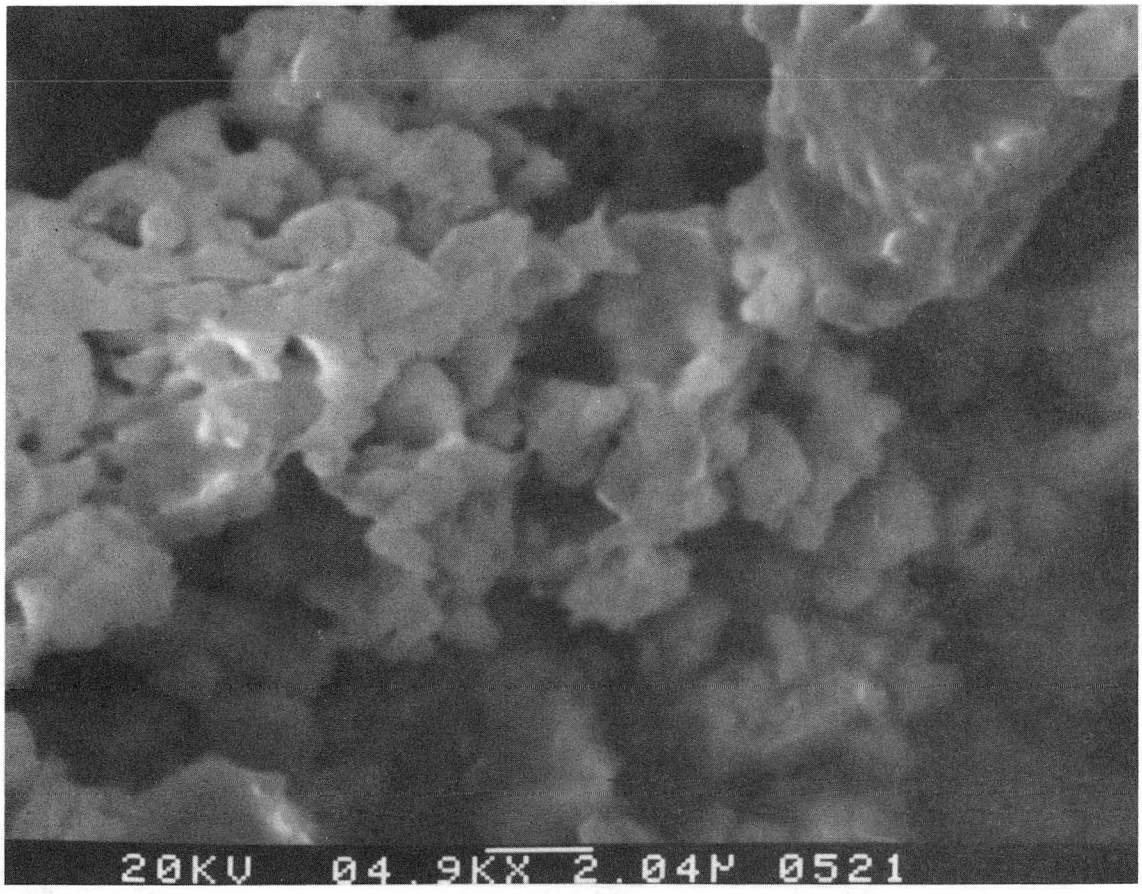

XBB 905-3682

Fig.9 SEM micrograph of synthesized powder (Mixed sample No.2)

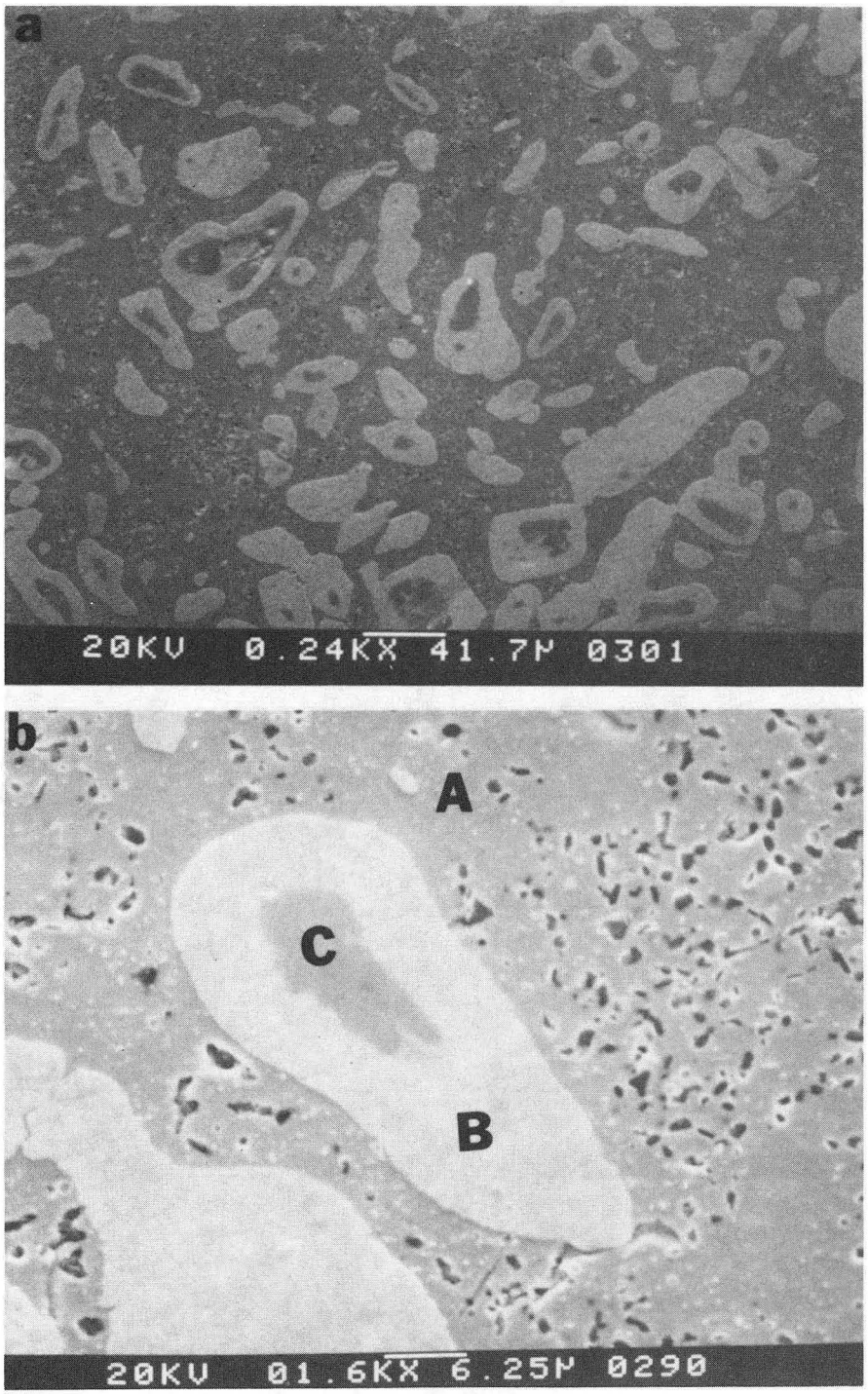

XBB 905-3681

Fig.10 SEM micrographs of the specimen 1. The specimen was hot pressed at 1700°C
(a) Low magnification.
(b) High magnification. EDXS analyses were carried out on regions (A), (B) and (C).

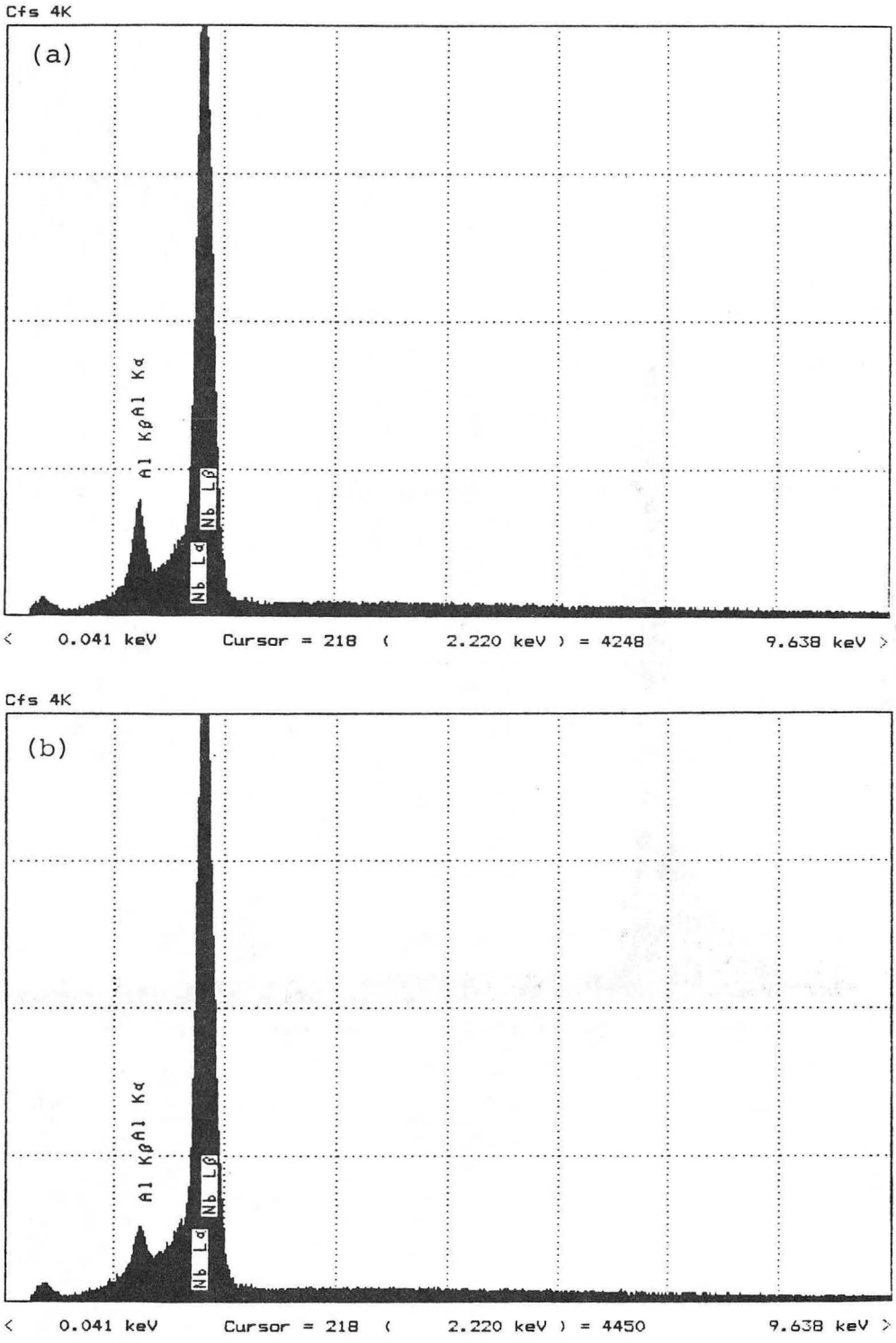

XBL 905-1704

Fig.11 EDXS analyses of the specimen 1.
(a) Obtained from region (A) in Fig.10(b).
(b) Obtained from region (B) in Fig.10(b).

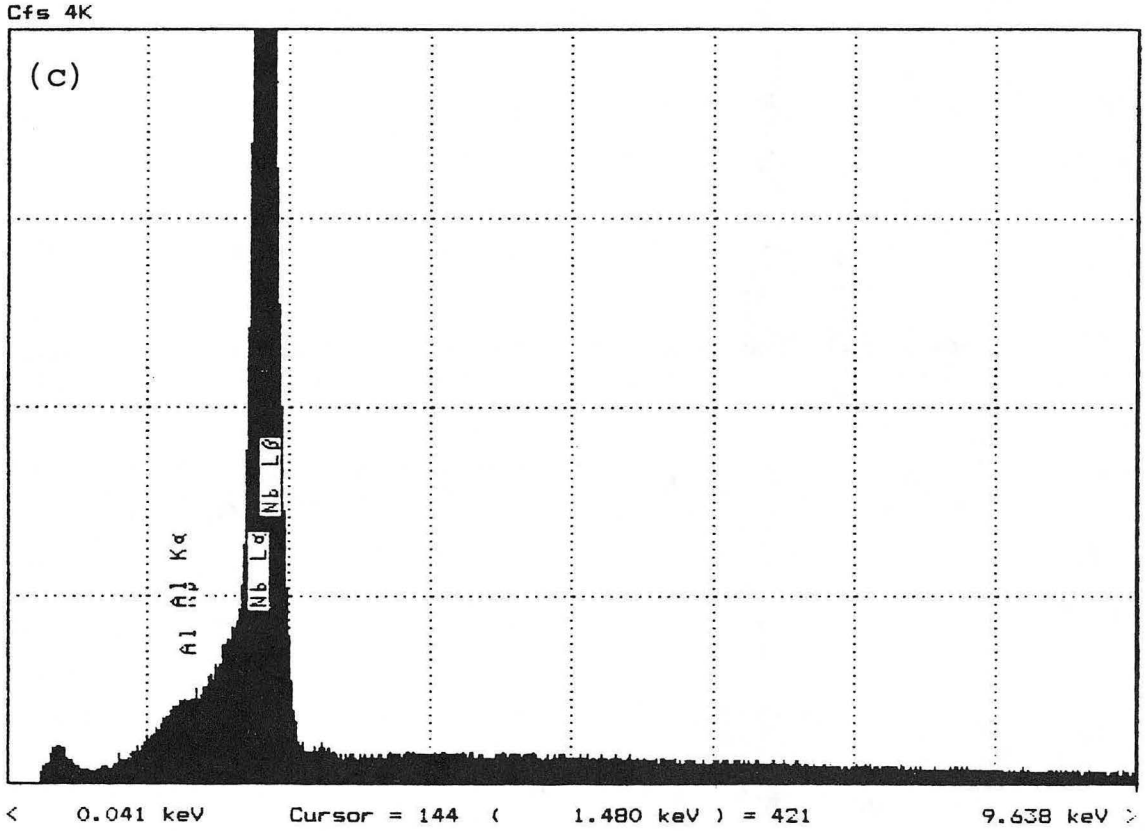

XBL 905-1713

Fig.11 (continued)
(c) Obtained from region (C) in Fig.10.

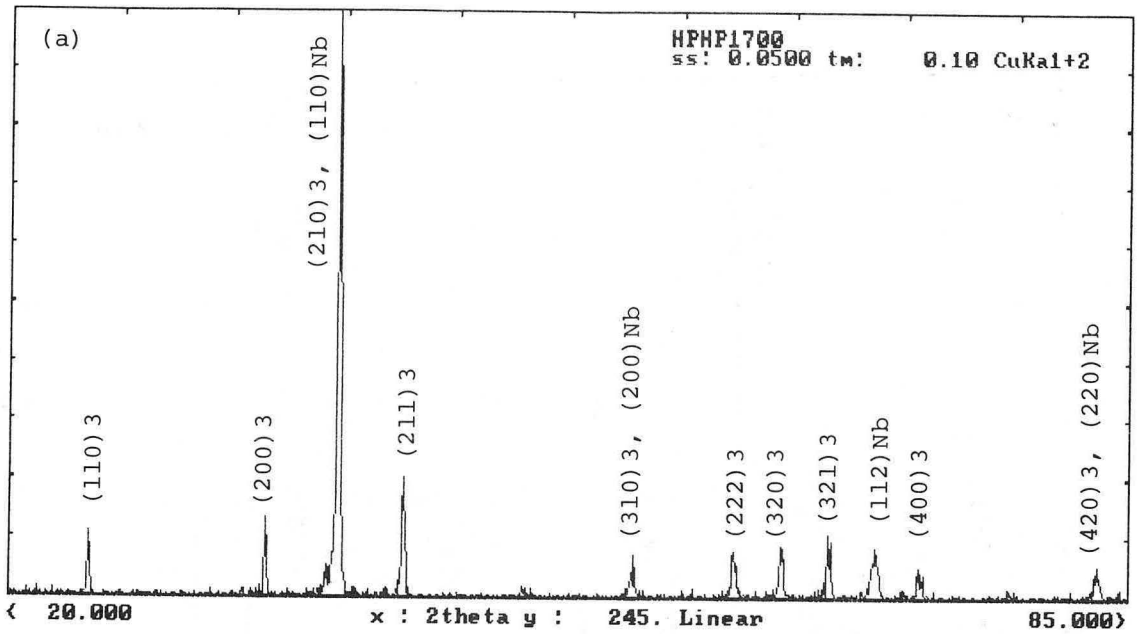

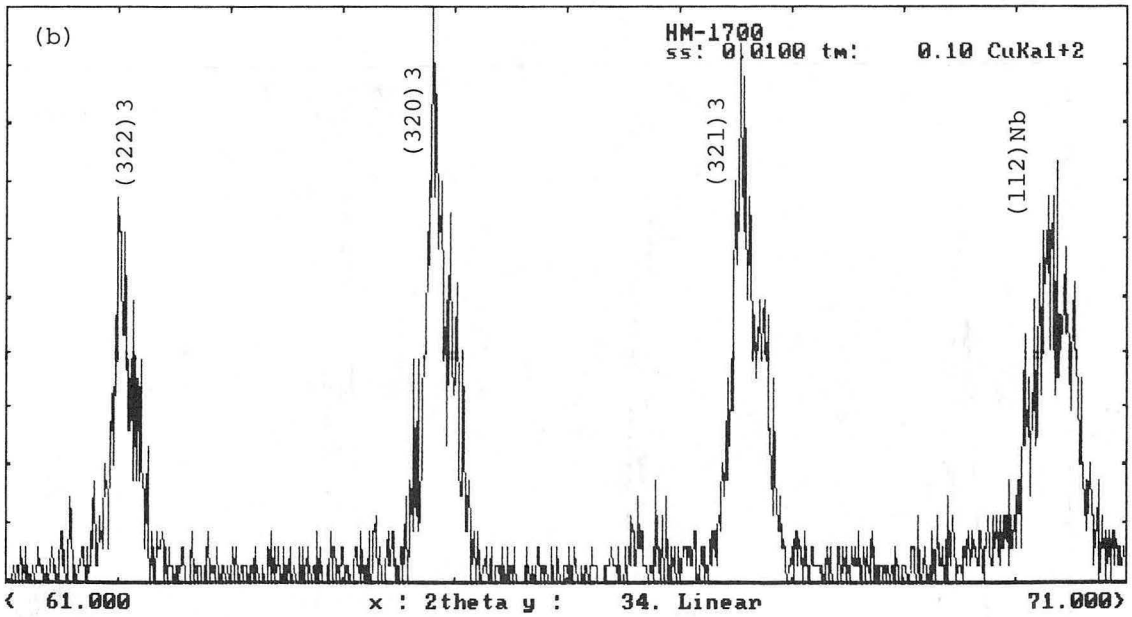

XBL 905-1710

Fig.12 X-ray diffraction patterns of the hot pressed specimen 1.
(a) 2θ range : 20 - 85°.
(b) 2θ range : 61 - 71°.
From the peak corresponding to (112)Nb, a slight shift of Nb peaks in the larger direction of 2θ is observed.
Standard peak position : 2θ = 69.87° (d = 1.375A)
Observed peak position : 2θ = 70.36° (d = 1.337A)

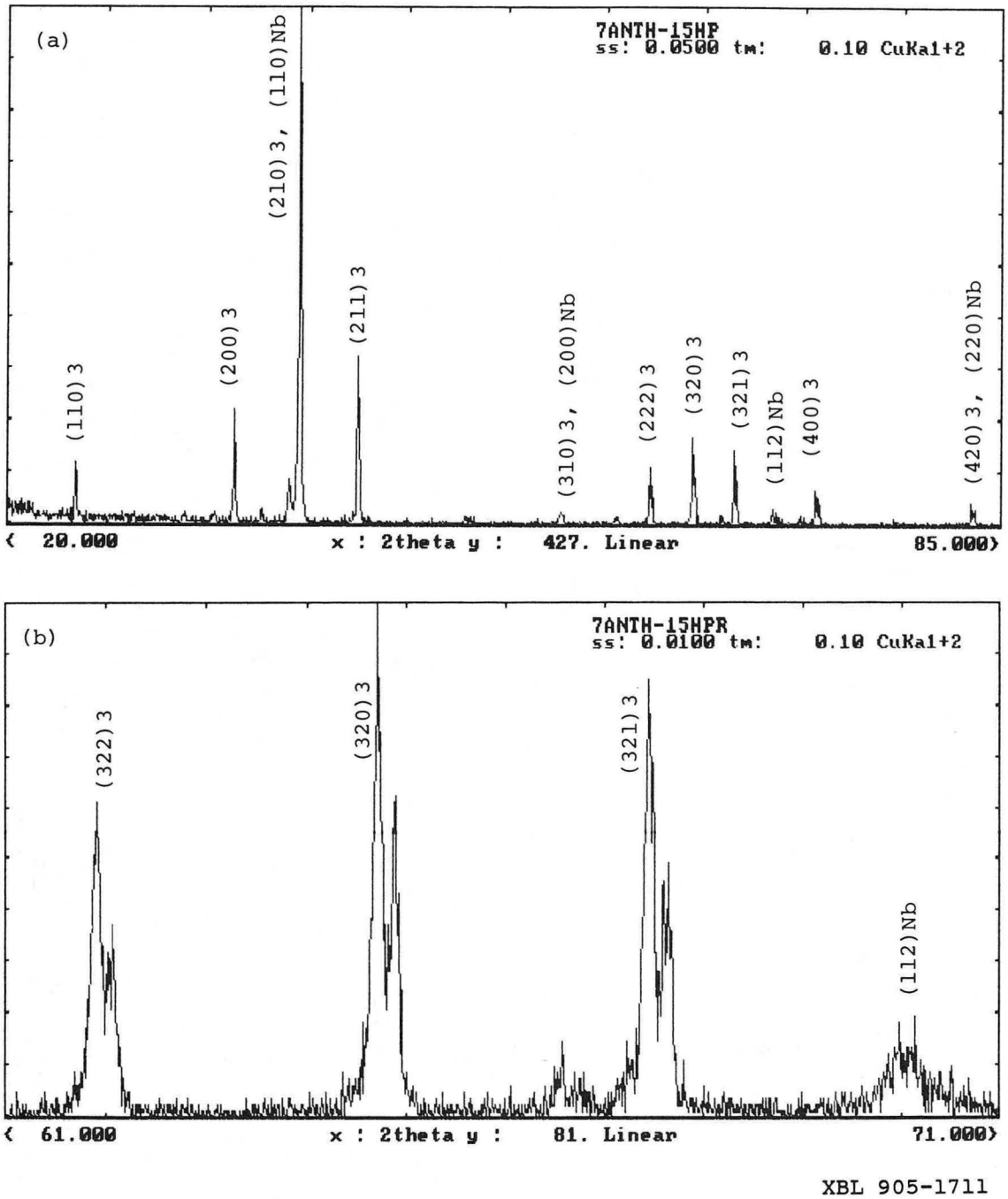

Fig.13 X-ray diffraction patterns of hot pressed specimen 2.
(a) 2θ range : 20 - 85°.
(b) 2θ range : 61 - 71°.

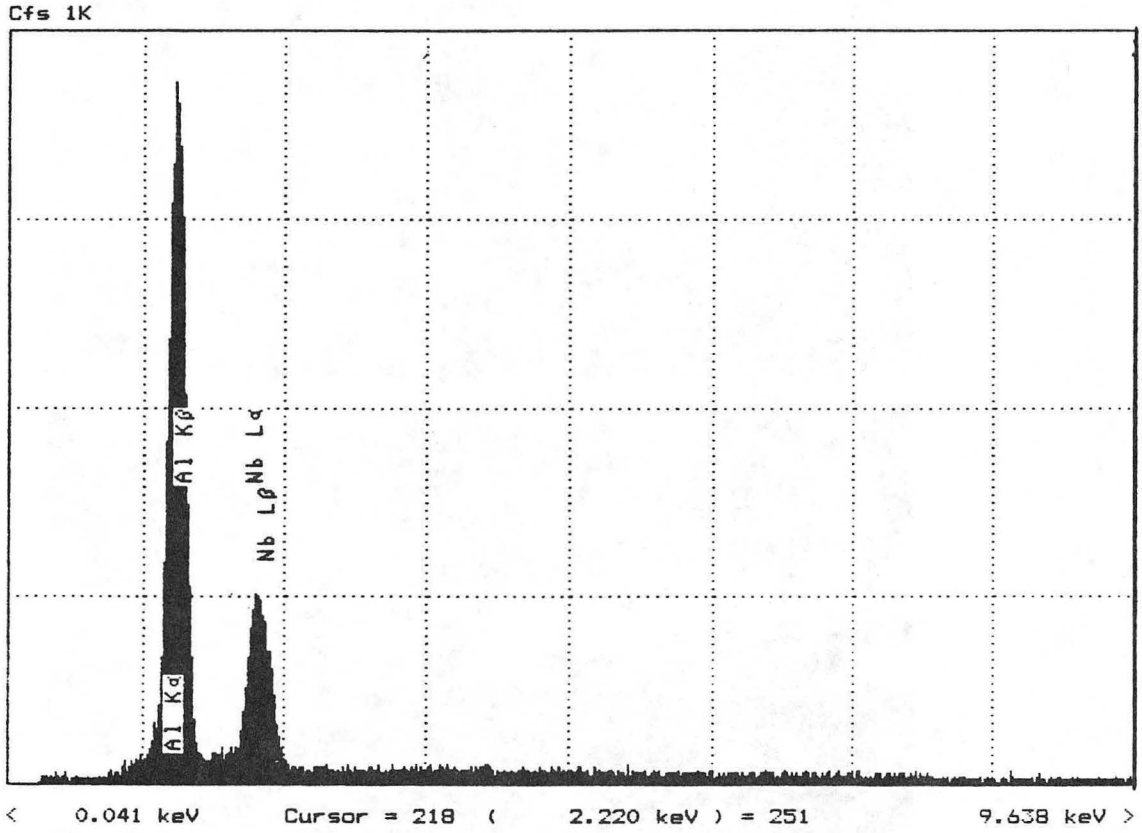

XBL 905-1714

Fig.14 EDXS analysis of hot pressed specimen 2. This result was obtained from the black particle commonly observed in the hot pressed specimens (cf. Fig.22).

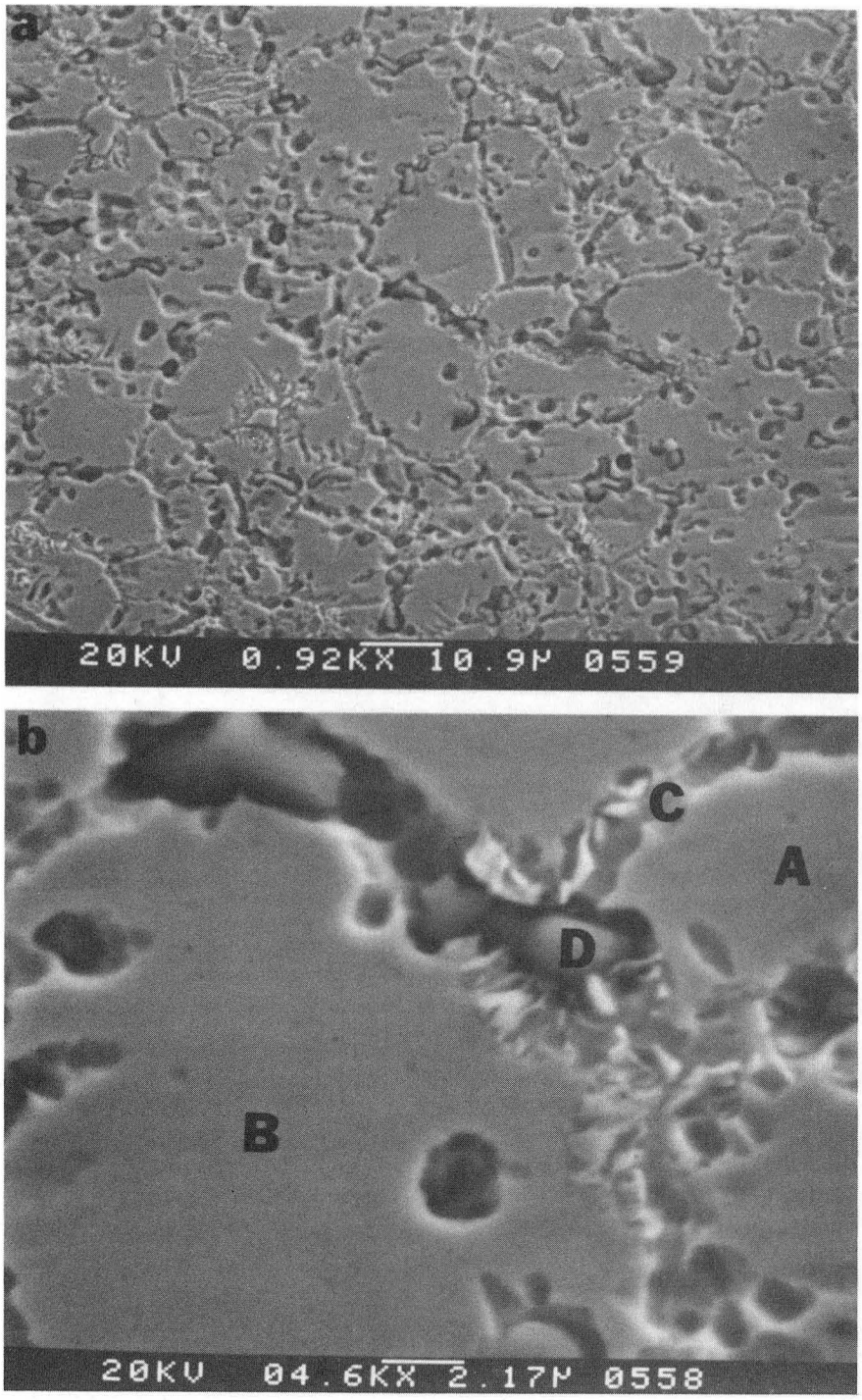

XBB 905-3680

Fig.15 SEM micrographs of hot pressed specimen 3. The composition of this specimen is 94wt% Nb.
(a) Low magnification
(b) High magnification
EDXS analyses were carried out on regions (A), (B), (C) and (D).

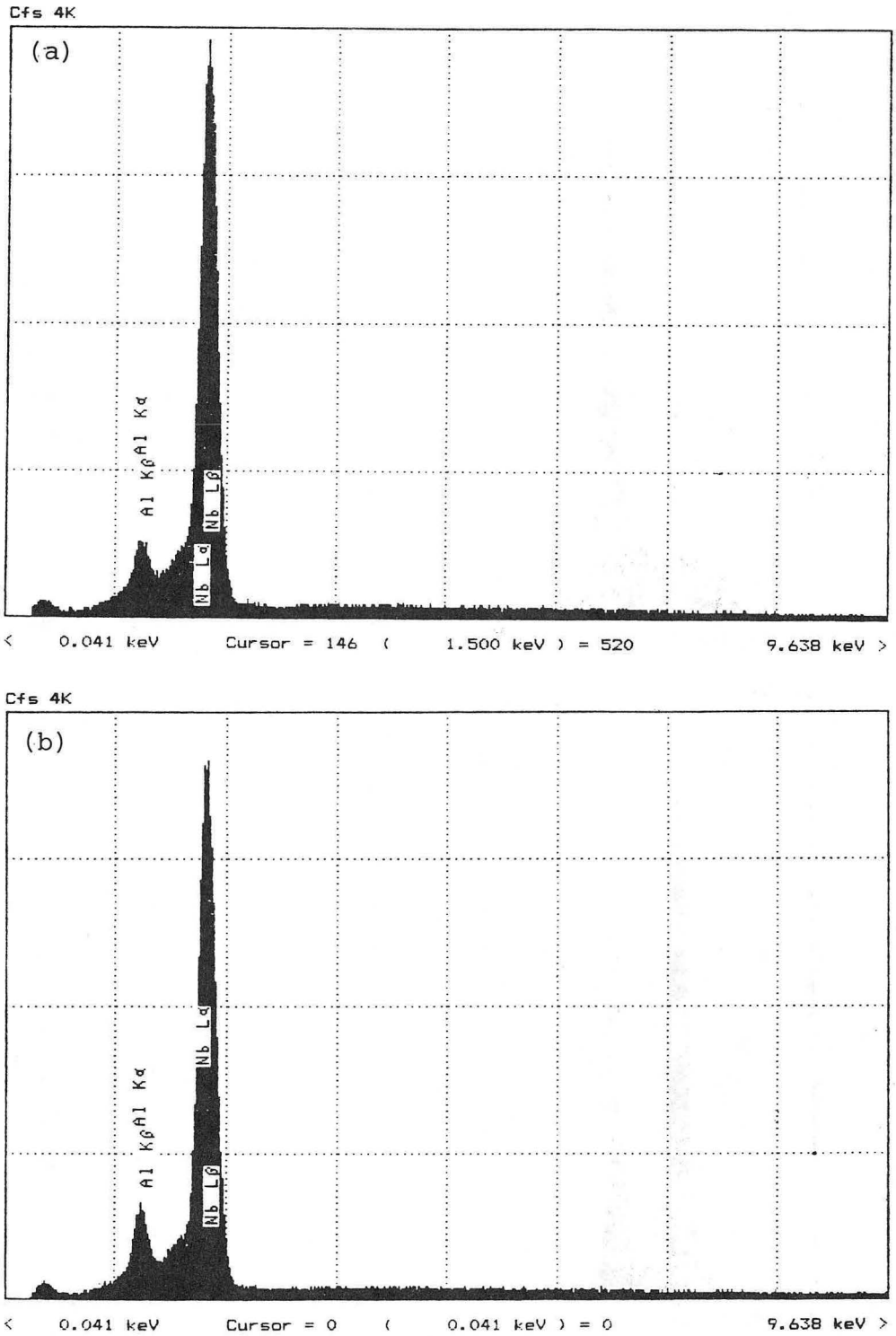

XBL 905-1706

Fig.16 EDXS analyses of hot pressed specimen 3.
(a) Obtained from region (A) in Fig.15(b).
(b) Obtained from region (B) in Fig.15(b).

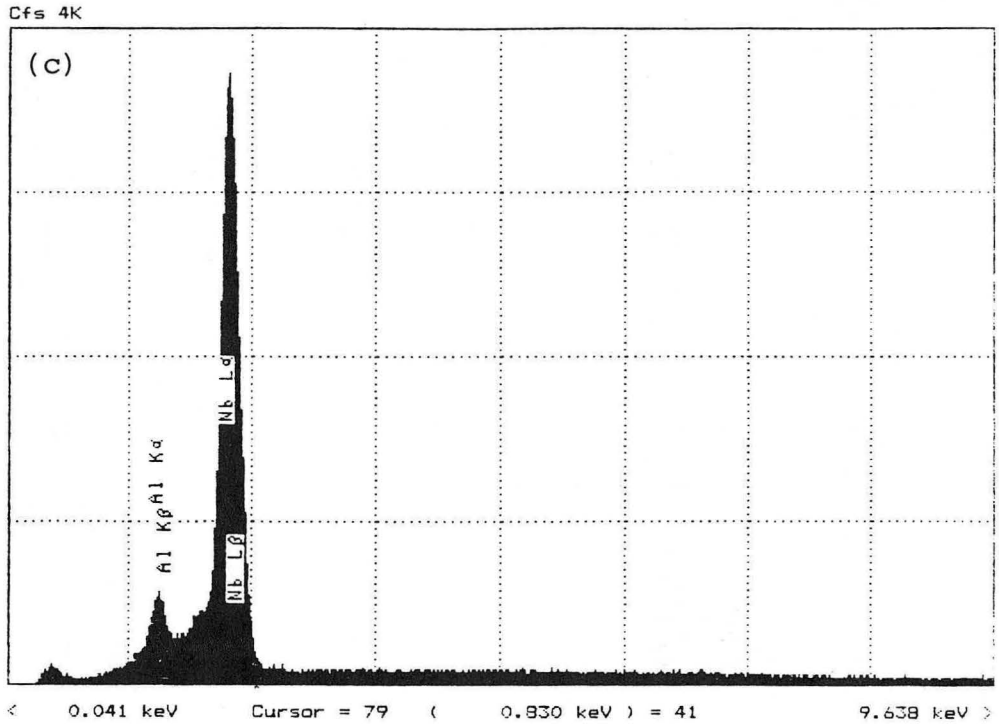

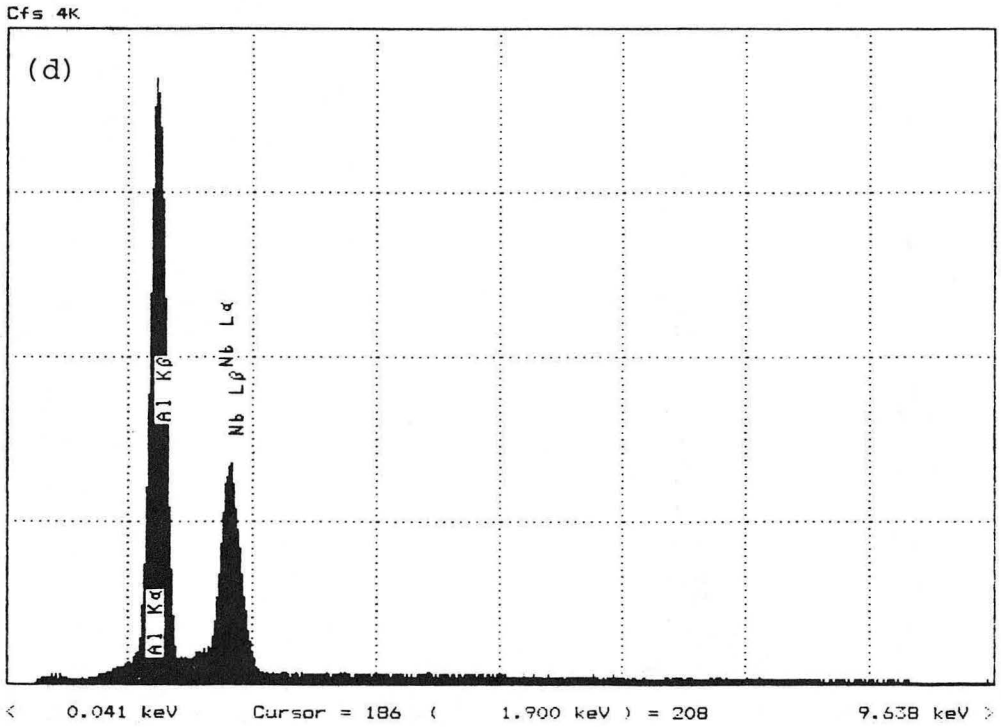

XBL 905-1705

Fig 16 (continued)
(c) Obtained from region (C) in Fig.15(b).
(d) Obtained from region (D) in Fig.15(b)

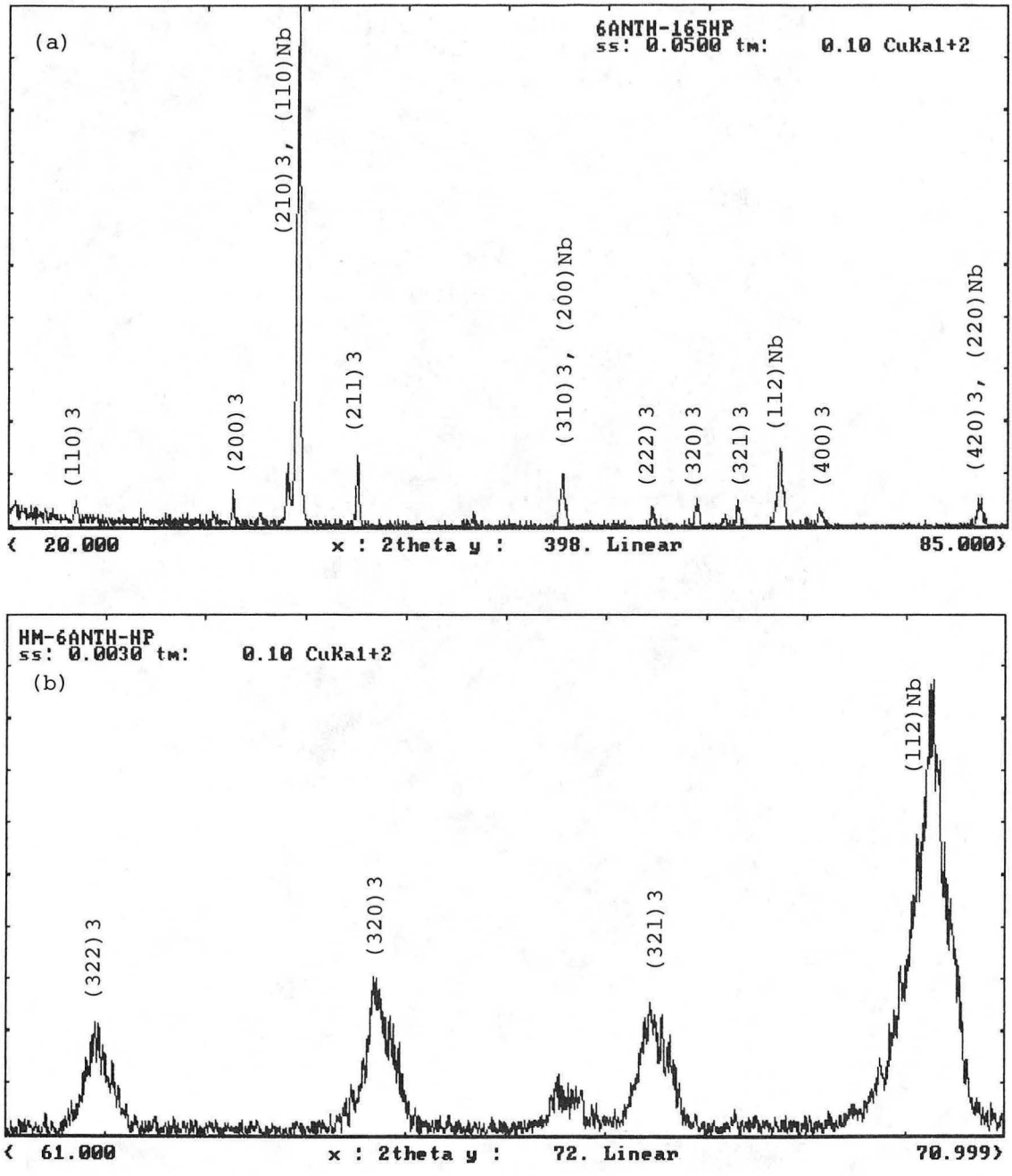

XBL 905-1712

Fig.17 X-ray diffraction patterns of hot pressed specimen 3.
(a) 2θ range : 20 - 85°.
(b) 2θ range : 61 - 71°.

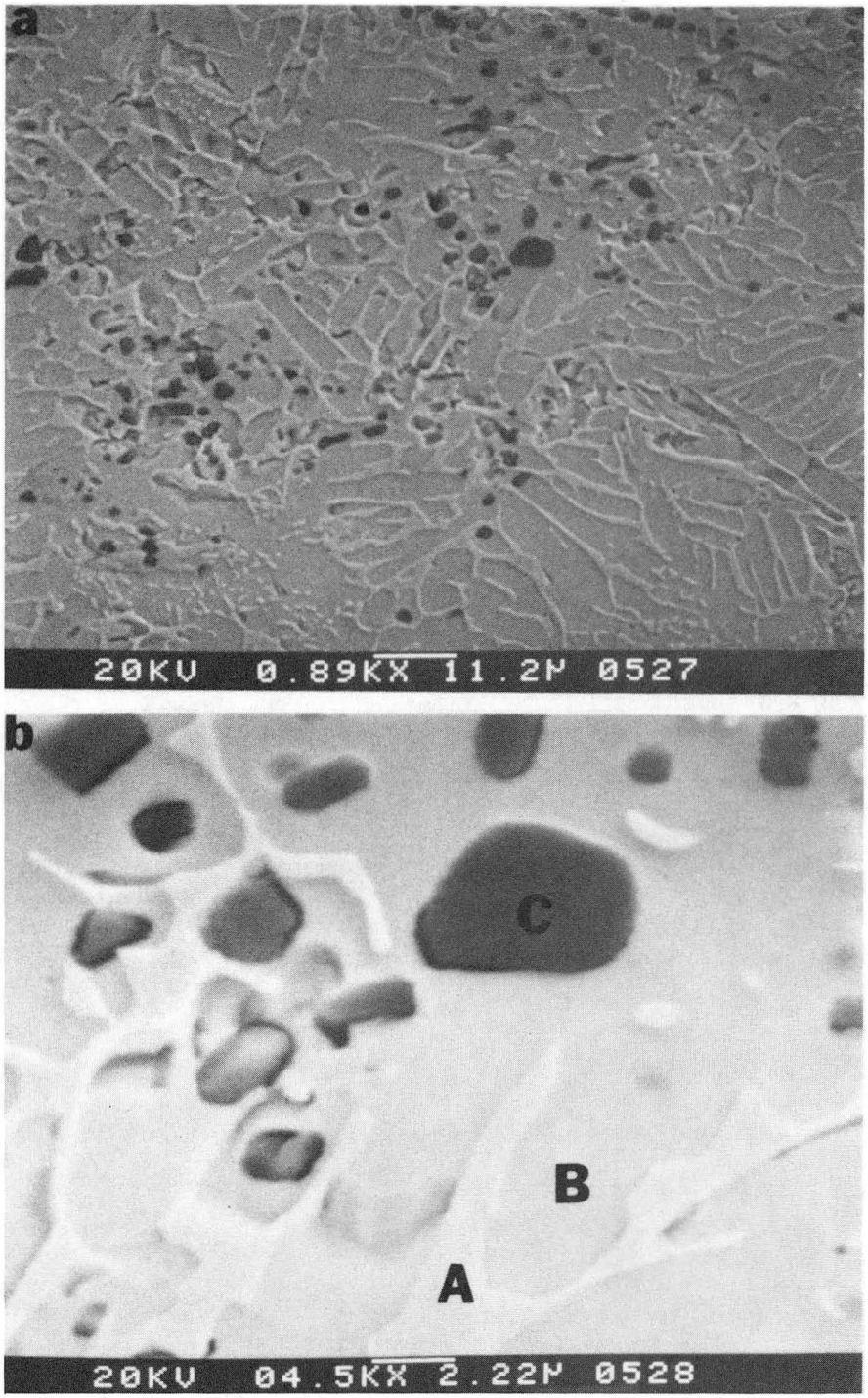

XBB 906-3679

Fig.18 SEM micrographs of heat treated specimen 1.
Heat treatment was carried out at 1800°C for 1Hr.
(a) Low magnification.
(b) High magnification.
EDXS analyses were carried out on regions (A), (B) and (C).

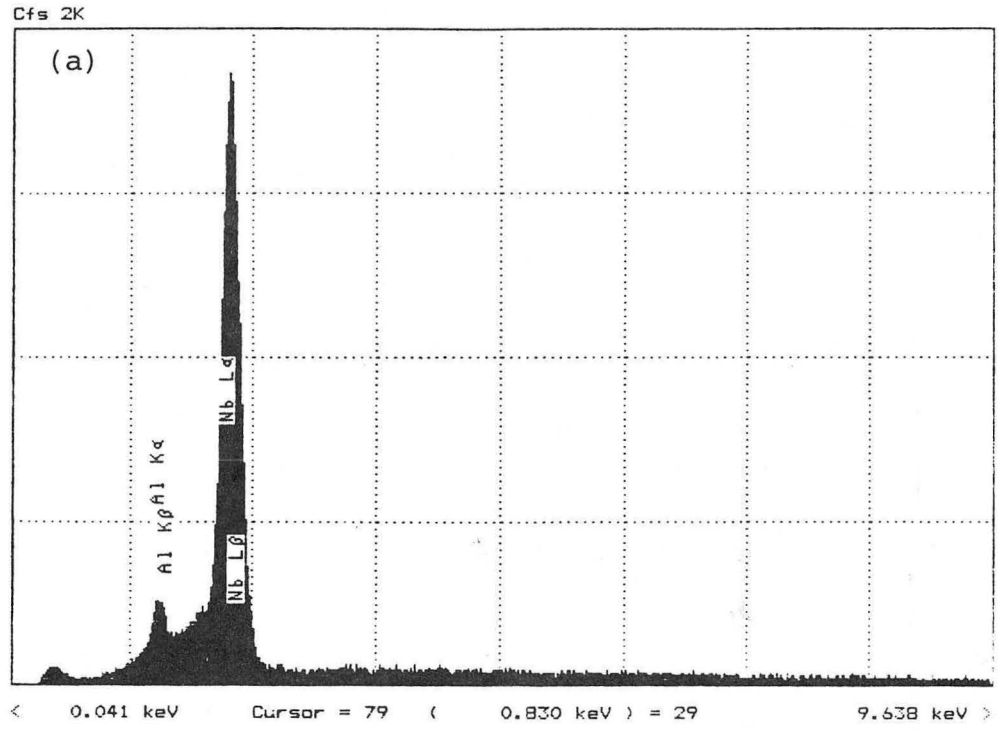

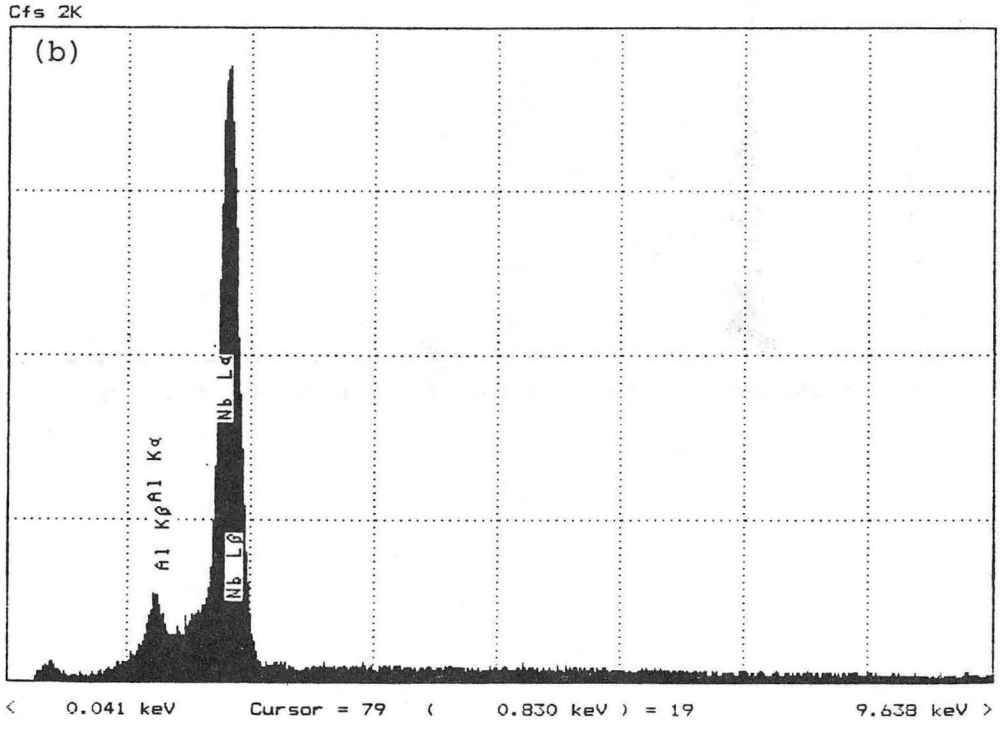

XBL 905-1703

Fig.19 EDXS analyses of heat treated specimen 1.
(a) Obtained from region (A) in Fig.18(b).
(b) Obtained from region (B) in Fig.18(b).

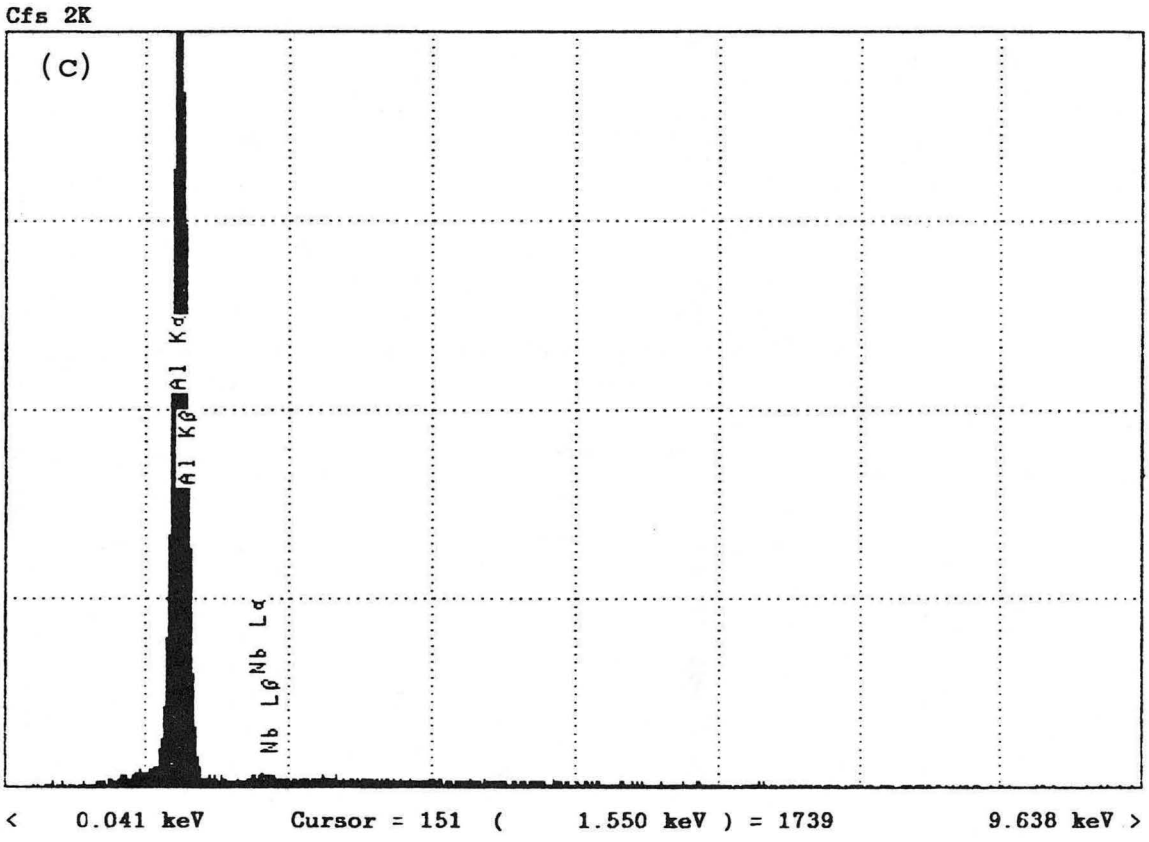

XBL 905-1715

Fig.19 (continued)
(c) Obtained from region (C) in Fig.18(b).

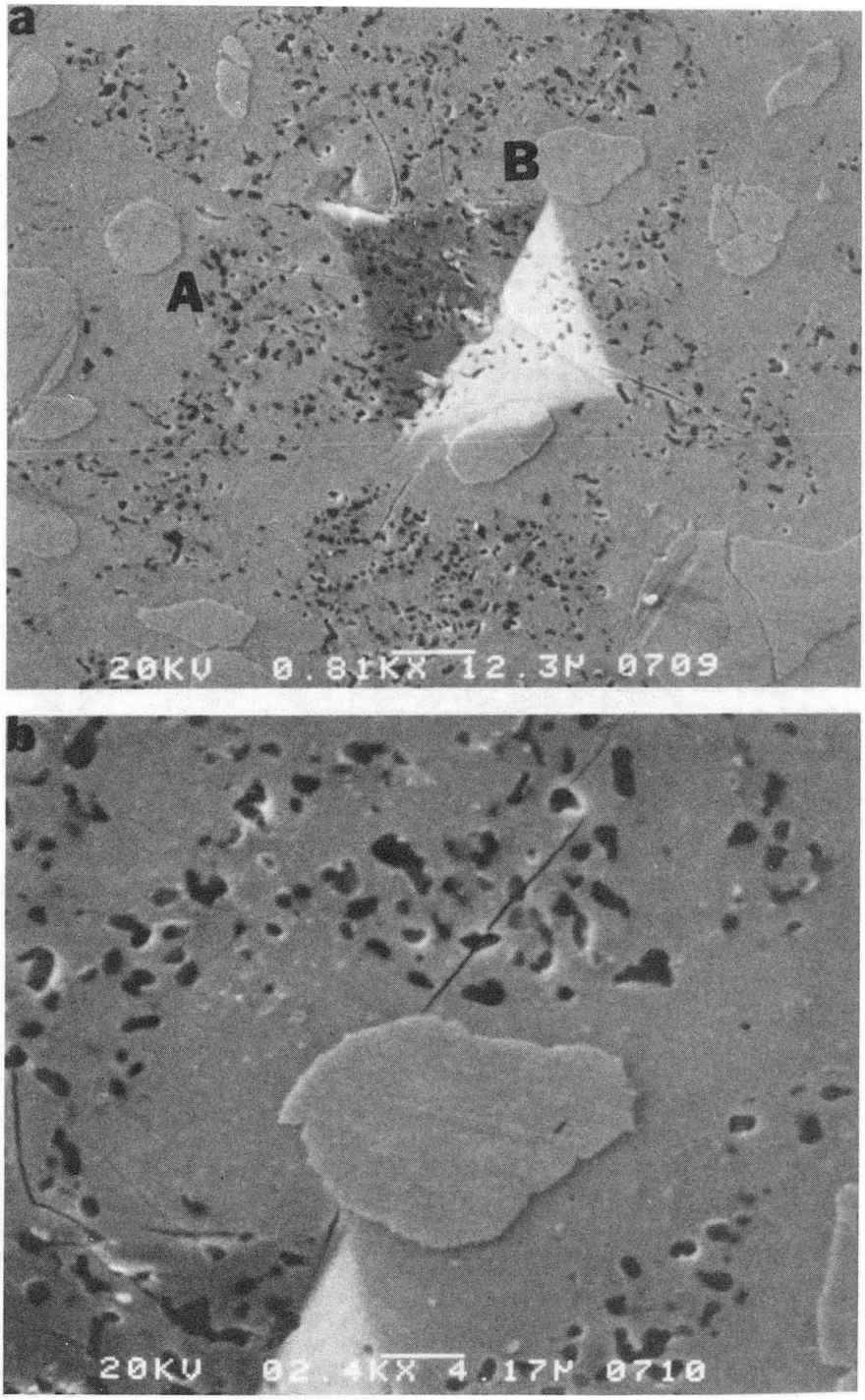

XBB 905-3678

Fig.20 Indentation results on hot pressed specimen 1.
Hv = 720.
(a) Low magnification.
(b) High magnification of region (B).
The crack is pinned by the Nb phase (A). The crack is propagating without penetrating the Nb phase (B).

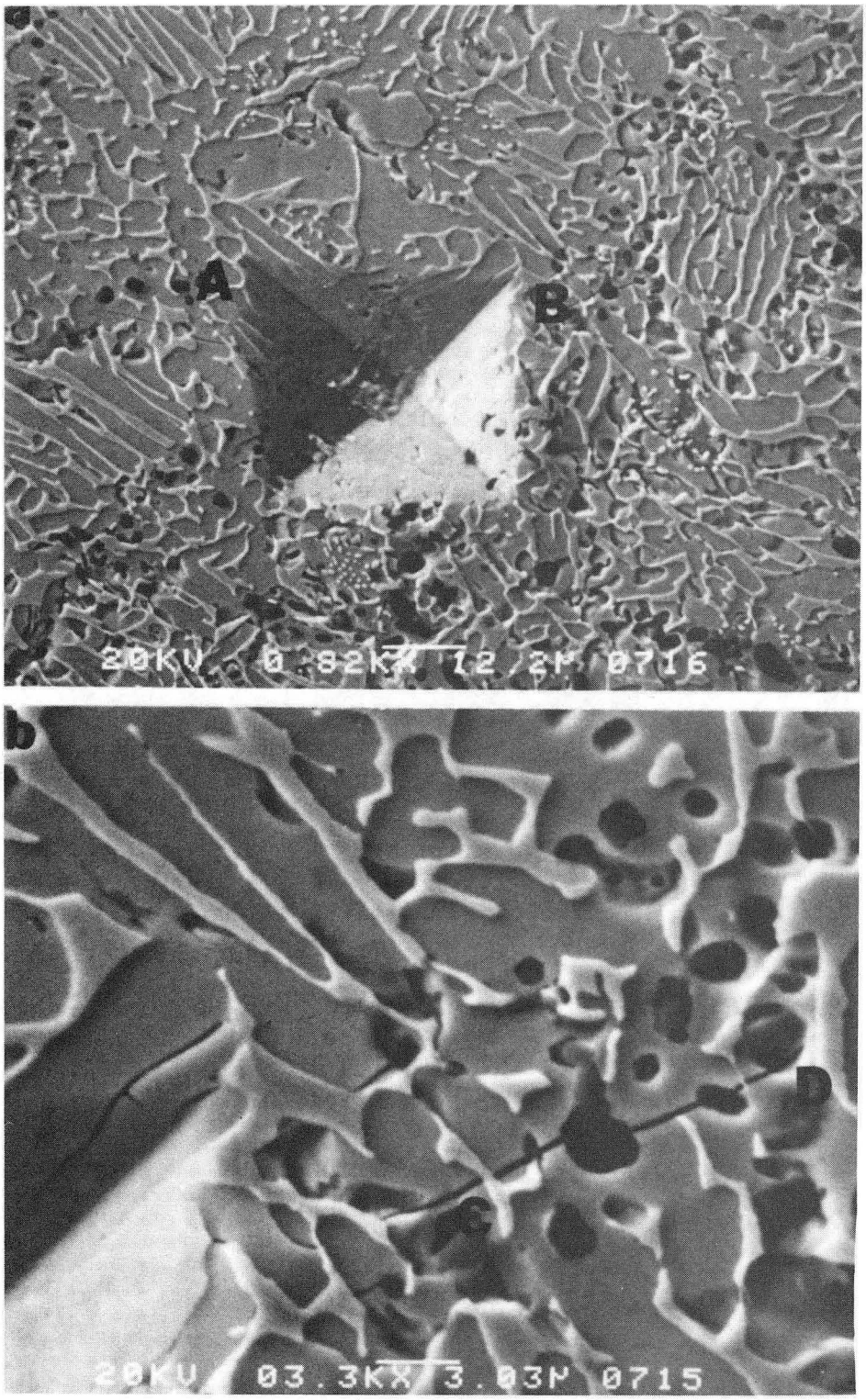

XBB 905-3677

Fig.21 Indentation results on heat treated specimen 1. heat treatment was carried out at 1700°C for 1Hr. Hv = 680.
(a) Low magnification.
(b) High magnification of the corner (B).

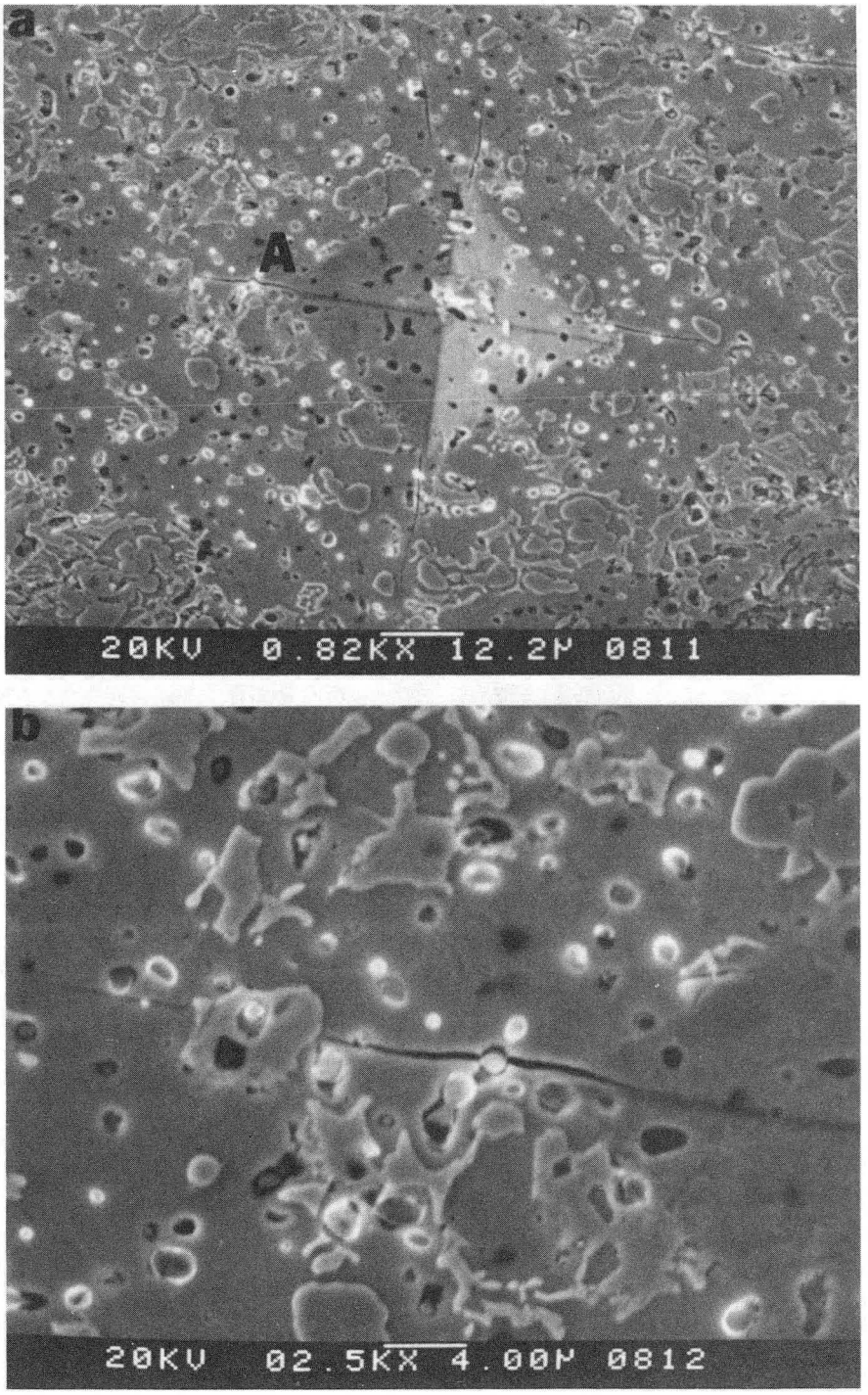

XBB 905-3676

Fig.22 Indentation results on hot pressed specimen 2.
Hv = 720.
(a) Low magnification.
(b) High magnification of the corner (A).

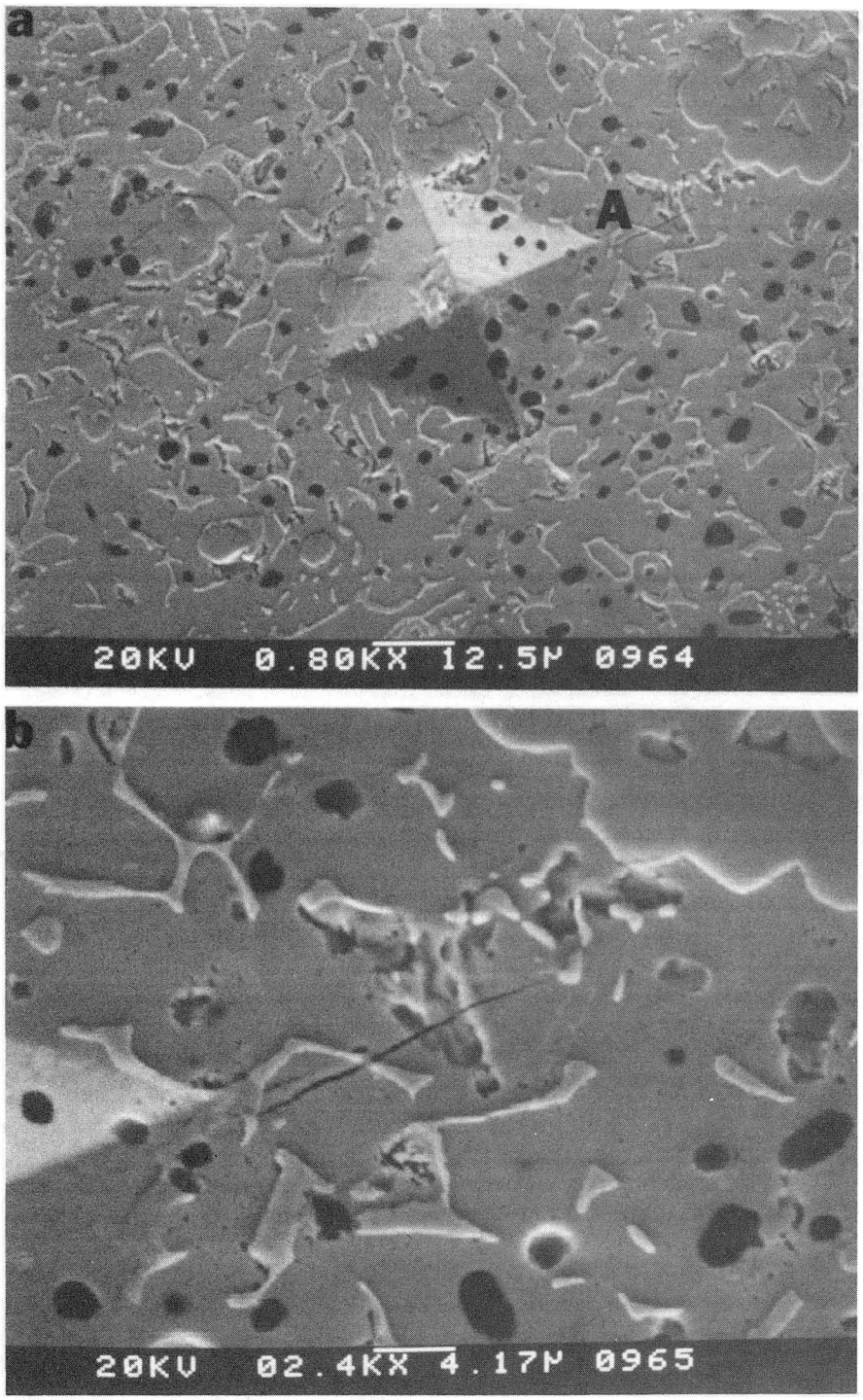

XBB 905-3675

Fig.23 Indentation results on heat treated specimen 2.
Heat treatment was carried out at 1750°C for 1Hr.
Hv = 710.
(a) Low magnification.
(b) High magnification of the corner (A).

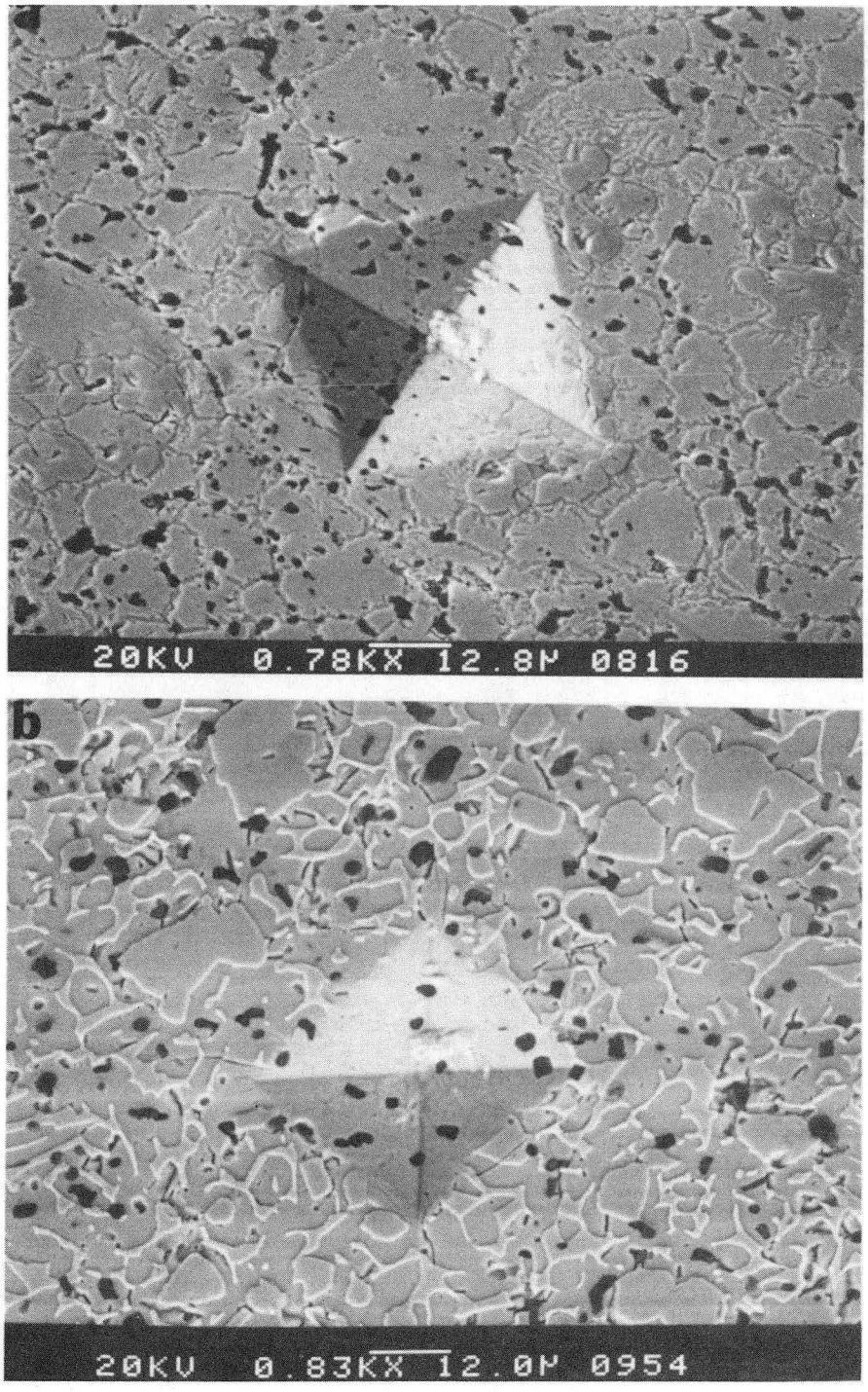

XBB 905-3674

Fig.24 Indentation results on the specimen 3.
(a) Hot pressed specimen. Hv = 540.
(b) Heat treated specimen at 1750°C. Hv = 780.

LAWRENCE BERKELEY LABORATORY
UNIVERSITY OF CALIFORNIA
INFORMATION RESOURCES DEPARTMENT
BERKELEY, CALIFORNIA 94720